3-2019

How crickets become freeze tolerant: the transcriptomic underpinnings of acclimation in Gryllus veletis

Jantina Toxopeus
Western University, jantina.toxopeus@ucdenver.edu

Lauren E. Des Marteaux
Western University, ldesmart@uwo.ca

Brent J. Sinclair
Western University, bsincla7@uwo.ca

How crickets become freeze tolerant: the transcriptomic underpinnings of acclimation in *Gryllus veletis*

Short title: **Transcriptomics of freeze tolerance**

Jantina Toxopeus[1,2]*, Lauren E. Des Marteaux[1,3], & Brent J. Sinclair[1]

[1]Department of Biology, University of Western Ontario, 1151 Richmond Street N, London, ON, Canada, N6A 5B7

[2]Present address: Department of Integrative Biology, University of Colorado, Denver, 1151 Arapahoe Street, Denver, CO, USA, 80204

[3]Present address: Biology Centre, Czech Academy of Sciences, Institute of Entomology, České Budějovice, Czech Republic 370 05

*Corresponding author: Department of Integrative Biology, University of Colorado, Denver, 1151 Arapahoe Street, Denver, CO, USA, 80204; email jantina.toxopeus@ucdenver.edu; tel 1-303-315-7670; fax 1-303-315-7601

Abstract

Some ectotherms can survive internal ice formation. In temperate regions, freeze tolerance is often induced by decreasing temperature and/or photoperiod during autumn. However, we have limited understanding of how seasonal changes in physiology contribute to freeze tolerance, and how these changes are regulated. During a six week autumn-like acclimation, late-instar juveniles of the spring field cricket *Gryllus veletis* (Orthoptera: Gryllidae) become freeze tolerant, which is correlated with accumulation of low molecular weight cryoprotectants, elevation of the temperature at which freezing begins, and metabolic rate suppression. We used RNA-Seq to assemble a *de novo* transcriptome of this emerging laboratory model for freeze tolerance research. We then focused on gene expression during acclimation in fat body tissue due to its role in cryoprotectant production and regulation of energetics. Acclimated *G. veletis* differentially expressed more than 3,000 transcripts in fat body. This differential expression may contribute to metabolic suppression in acclimated *G. veletis*, but we did not detect changes in expression that would support cryoprotectant accumulation or enhanced control of ice formation, suggesting that these latter processes are regulated post-transcriptionally. Acclimated *G. veletis* differentially regulated transcripts that likely coordinate additional freeze tolerance mechanisms, including upregulation of enzymes that may promote membrane and cytoskeletal remodelling, cryoprotectant transporters, cytoprotective proteins, and antioxidants. Thus, while accumulation of cryoprotectants and controlling ice formation are commonly associated with insect freeze tolerance, our results support the hypothesis that many other systems contribute to surviving internal ice formation. Together, this information suggests new avenues for understanding the mechanisms underlying insect freeze tolerance.

Key words

acclimation; cold tolerance; freeze tolerance; insect; RNA-Seq; transcriptomics

Introduction

Many insects that overwinter in temperate regions risk freezing of their body fluids. Insects survive these low temperatures using a range of physiological strategies, including freeze avoidance (depressing the temperature at which body fluids freeze), cryoprotective dehydration (decreasing the amount of freezable water in the body), vitrification (preventing ice crystallization by transitioning body fluids to a "glass" state), and freeze tolerance (surviving internal ice formation; Lee, 2010). Freeze-tolerant insects must survive a combination of challenges, including those imposed by low temperatures, internal ice, and metabolic limitations (Toxopeus and Sinclair, 2018). Low temperatures alone can cause injury, such as cell death associated with membrane depolarization (Bayley et al., 2018). Low temperatures and freezing are hypothesized to damage cellular macromolecules *via* cold- or dehydration-induced protein denaturation or membrane phase transitions (Hazel, 1995; Rinehart et al., 2006; Dias et al., 2010), accumulation of oxidative damage (Doelling et al., 2014; Lalouette et al., 2011), and build-up of toxic metabolites (e.g. lactate) over time (Storey and Storey, 1985). For example, freezing can cause dissociation and damage of cytoskeletal proteins in fat body of the drosophilid fly *Chymomyza costata* (Des Marteaux et al., 2018a). In addition, ice formation and recrystallization (ice crystal growth at equilibrium ice content) may mechanically damage cells and tissues (Pegg, 2010). We have previously hypothesized that five broad mechanisms contribute to freeze tolerance (Toxopeus and Sinclair, 2018): freeze-tolerant insects may 1) control the process of ice formation and propagation, 2) reduce ice content, 3) stabilize cells and macromolecules, 4) prevent accumulation of harmful metabolites, and 5) coordinate repair and recovery post-thaw. However, the regulation of these mechanisms and the extent to which they facilitate freeze tolerance is unknown.

Many temperate insects become freeze tolerant as winter approaches, and descriptive studies have identified biochemical and molecular correlates that could facilitate this cold tolerance strategy (Lee, 2010). For example, freeze-tolerant insects can seasonally alter macromolecule composition (membranes and proteins), and accumulate low molecular weight cryoprotectants, cytoprotective proteins, ice-binding molecules, and aquaporins (AQPs; Toxopeus and Sinclair, 2018). Altering macromolecule composition (e.g. membranes; Koštál et al., 2003) may reduce macromolecule damage due to low temperatures and ice. Low molecular weight cryoprotectants

such as sugars, polyols, and amino acids (Lee, 2010), and potentially cyto- and cryo-protective proteins such as heat shock proteins (HSPs; Lu et al., 2014; Zhang et al., 2011) can also protect cells and macromolecules at low temperatures. Ice-binding molecules may reduce mechanical damage from ice: ice-nucleating agents (INAs) can control where and when ice begins to form, and many antifreeze proteins (AFPs) can inhibit ice recrystallization (Zachariassen et al., 2004; Duman, 2015). Similarly, AQPs may help control ice location by facilitating osmotic dehydration of cells during freezing, thereby preventing intracellular ice formation (IIF; Philip and Lee, 2010; Yi et al., 2011). Freeze-tolerant insects may also suppress their metabolic rate (e.g. in diapause; Irwin and Lee, 2002), which could reduce metabolic dysregulation in the frozen state.

Despite the diversity of molecules that may contribute to freeze tolerance, we have limited understanding of the pathways that regulate seasonal changes and have explored only a narrow range of other cellular and physiological processes during acclimation that may contribute to freeze tolerance. Many seasonally-induced physiological changes (e.g. entry into diapause) are regulated by hormones, including juvenile hormone (JH; Sim and Denlinger, 2013), 20-hydroxyecdysone (20HE; Poupardin et al., 2015; Koštál et al., 2017) and insulin signalling (Sim and Denlinger, 2008; Koštál et al., 2017; Sinclair and Marshall, 2018), but whether these initiate freeze tolerance is undetermined. Seasonal changes in enzyme activity may account for cryoprotectant accumulation in *Eurosta solidaginis* (Joanisse and Storey, 1994; Storey and Storey, 1981), but the mechanisms underpinning other changes (e.g. membrane composition) are less clear. Untargeted '-omics' (e.g. metabolomics, transcriptomics) studies of freeze-tolerant insects to date have identified acute responses to cooling, freezing, or dehydration (Courteau et al., 2012; Teets et al., 2012a; Teets et al., 2013; Dennis et al., 2015; Štětina et al., 2018), but few have documented the changes associated with seasonal acquisition of freeze tolerance (Poupardin et al., 2015). Some genes that are seasonally upregulated in freeze-tolerant insects (e.g. HSPs, AQPs) have been identified *via* targeted studies (Philip and Lee, 2010; Yi et al., 2011; Zhang et al., 2011; Lu et al., 2014), but few other genes (e.g. those encoding ice-binding proteins; Duman, 2015) have been linked to the acquisition of freeze tolerance.

The spring field cricket, *Gryllus veletis* (Orthoptera: Gryllidae), is a promising model for mechanistic studies of insect freeze tolerance (Toxopeus et al., submitted). A laboratory acclimation that mimics autumn (six weeks of decreasing temperature and photoperiod) induces freeze tolerance in late instar juveniles, which are freeze tolerant when overwintering in nature (Toxopeus et al., submitted). Like many other insects, this acquisition of freeze tolerance is accompanied by increased hemolymph osmolality (e.g. due to accumulation of low molecular weight cryoprotectants), increased control of ice nucleation (elevated supercooling point, SCP; the temperature at which ice formation begins), and reduced metabolic rate (Toxopeus et al., submitted). Here we assembled a transcriptome for *G. veletis* and compared gene expression in the fat body tissue of fifth instar males during six weeks of acclimation or control conditions. We chose to examine the fat body because of its role in regulation of energetics and cryoprotectant production (Arrese and Soulages, 2010). We aimed to determine which pathways regulate the physiological changes associated with freeze tolerance, and to identify previously unexplored cellular processes that may contribute to the mechanisms underlying freeze tolerance.

Materials and Methods

Study animals

Our laboratory colony of *G. veletis* originated from individuals collected in 2010 from the University of Lethbridge campus, Alberta, Canada. We reared the crickets at 25ºC, 14:10 L:D photoperiod, 70% RH, as described previously (Toxopeus et al., submitted). Approximately eight weeks post-hatch, we isolated fifth instar male nymphs into individual mesh-covered 180 mL transparent cups (Polar Plastics, Summit Food Distributors, London, ON, Canada) containing egg carton shelters, rabbit food, and water. We then haphazardly assigned crickets to either remain in rearing (control) conditions for six weeks (25ºC, 14:10 L:D), or to undergo a six week acclimation mimicking autumn conditions. We acclimated crickets in a Sanyo MIR 154 incubator (Sanyo Scientific, Bensenville, IL, USA), with photoperiod decreasing from 11.5:12.5 L:D to 7.9:16.1 L:D and fluctuating temperatures decreasing from 16/12ºC (12 h at each high/low temperature) to 1/0ºC over six weeks. This regime induces freeze tolerance in *G. veletis* nymphs, while nymphs maintained under control conditions are freeze-intolerant (Toxopeus et al., submitted).

RNA extraction, cDNA library preparation, and sequencing

We dissected fat body tissue for RNA extraction after zero, three, and six weeks of control or acclimation conditions. At zero weeks we collected tissue from control crickets only. At three and six weeks we collected tissue from control and acclimated crickets. We briefly blotted fat body samples on tissue paper to remove hemolymph, transferred them to 1.7 mL microcentrifuge tubes, and flash froze the samples in liquid nitrogen. Each biological replicate was comprised of fat body tissue pooled from five males from the same cohort. To limit variability introduced by sex, we did not collect tissue from female crickets. We generated mRNA libraries for three biological replicates of each treatment, representing three cohorts of crickets (15 libraries total). To maximize the breadth of transcript representation for the *de novo* assembly, we extracted RNA from an additional *G. veletis* sample including tissues pooled from various developmental stages: whole male and female adult crickets, first through fifth instar nymphs, fifth instar nymphs that had undergone chilling (0°C for 1, 4, and 24 h), freezing (-8°C for 1.5 h), thawing, dehydration (incubation at room temperature with silica gel for 1, 4, and 24 h), and an immune challenge (injection with heat-killed bacteria, recovery for 1, 6, and 24 h). All samples were stored at -80ºC until RNA extraction.

We homogenized each of the 16 tissue samples with a plastic micropestle in TRIzol (ThermoFisher Scientific, Mississauga, ON, Canada) and extracted RNA according to manufacturer's instructions. We purified RNA extracts using the GeneJet RNA Cleanup & Concentration Micro Kit (ThermoFisher Scientific) according to manufacturer's instructions and measured absorbance at 260 nm to determine the RNA concentration. Génome Québec (Montréal, QC, Canada) conducted quality analysis on each sample with an Agilent Bioanalyzer, prepared KAPA/NEB stranded cDNA libraries from mRNA transcripts, and performed paired-end, 125 bp sequencing on the Illumina HiSeq 2500 platform (Illumina, San Diego, CA, USA).

De novo *transcriptome assembly and annotation*

We assembled the *G. veletis* transcriptome using a pipeline similar to that described previously (Des Marteaux et al., 2017). Briefly, we removed Illumina adapter sequences and discarded sequences shorter than 15 nucleotides or containing unknown bases using Cutadapt (Martin, 2011). We grouped trimmed sequences from all 16 libraries and assembled *de novo* an initial

transcriptome with a minimum contig length of 200 nucleotides using Trinity v2.2.0 (Grabherr et al., 2011; Haas et al., 2013) on the SHARCNET computing cluster (https://www.sharcnet.ca). We compared transcriptome assembly 'completeness' to a database (October 2016) of arthropod Benchmark Universal Single Copy Orthologs (BUSCO) using BUSCO v1.22 (Simão et al., 2015). We used Trinotate v3.0.1 on the SHARCNET computing cluster to assign putative identities to each contig from the Trinity assembly using BLASTx and BLASTp with an e-value threshold = 1×10^{-3} (Altschul et al., 1990) against the UniProt database (September 2016). We also used Trinotate to identify GO (Gene Ontology) terms (Ashburner et al., 2000), KEGG (Kyoto Encyclopedia of Genes and Genomes) terms (Kanehisa et al., 2011), and Pfam (protein family) domains (Punta et al., 2011) associated with each contig.

Differential gene expression analysis

To determine contig (putative transcript) read counts in each library, we first mapped the original cleaned sequence reads back onto the Trinity-assembly using Bowtie2 v2.2.9 (Langmead and Salzberg, 2012; Li et al., 2009b) and reassembled them with the Cufflinks package v2.2.1 (Trapnell et al., 2012) to filter out transcriptional artifacts, misassembled transcripts, and poorly supported transcripts. We then quantified contig abundance using HTSeq v0.6.1p1 (Anders et al., 2015), and normalized read counts for differential gene expression analysis using the edgeR Bioconductor package (Robinson et al., 2010) in R v3.4.1 (Risso et al., 2014; R Core Team, 2017).

To compare expression patterns over time between control and acclimated crickets, we used the maSigPro Bioconductor package (Conesa et al., 2006) in R to identify differentially expressed transcripts (with at least one read count in half of the libraries) and cluster them into nine expression patterns using a stepwise regression function. We used the same zero-week samples for both control and acclimated crickets in the analysis. This approach revealed that gene expression changed over six weeks in both control and acclimation conditions. As a result, we approached age-matched pairwise comparisons indirectly in subsequent analyses by comparing each group to the zero week control. We avoided direct age-matched pairwise comparisons because of their potential to be misleading. If (for example) control crickets upregulated a transcript after six weeks but acclimated crickets did not differentially express that same

transcript, comparing the control and acclimated groups at the six week time point would (incorrectly) suggest that acclimated crickets actively downregulated that gene.

To identify processes that were up- or down-regulated during acclimation, we conducted GO enrichment analysis using the goseq Bioconductor package (Young et al., 2010) in R on contigs identified as differentially regulated by maSigPro. We did pairwise comparisons of each treatment group relative to the zero week control, and accepted GO terms as over- or under-represented if the FDR-adjusted *P*-value was < 0.1, and if there were more than three transcripts representing that GO term. Redundant GO terms were removed with REViGO (Supek et al., 2011), using the SimRel algorithm, allowing medium similarity. We also identified differentially-enriched KEGG pathways in each treatment group relative to the zero week control using the Generally Applicable Gene-set Enrichment (GAGE) and Pathview Bioconductor packages (Luo and Brouwer, 2013; Luo et al., 2009) in R. These packages identify coordinated differential expression in gene sets (pre-defined, functionally-related groups of genes; Luo et al., 2009). We accepted pathways as differentially-expressed if the FDR-adjusted *P*-value was < 0.1.

Results and Discussion

Transcriptome summary

We assembled 672 million 125-bp paired-end reads from 16 libraries into a reference transcriptome (see Table 1 for detailed description). The transcriptome included 77.6 % complete arthropod BUSCOs, which is similar to or better than other recent arthropod *de novo* transcriptome assemblies (Tassone et al., 2016; Theissinger et al., 2016; Des Marteaux et al., 2017). Approximately 28,000 contigs (putative transcripts) were annotated, of which 97 % were assigned identities based on BLAST matches to the UniProt database, 88 % had GO terms, 47 % had KEGG IDs, and 65 % had identifiable Pfam domain(s) (Table 1). Our analysis focuses primarily on these annotated transcripts, although we speculate that subsequent exploration of unannotated transcripts may reveal novel factors associated with freeze tolerance.

Differential gene expression in early and late acclimation may contribute to freeze tolerance

A total of 3,306 putative transcripts were differentially-regulated in fat body tissue from juvenile *G. veletis* males during six weeks of control or acclimation conditions, each clustering into one

of nine differential expression patterns (Fig. 1). This differential expression resulted in over- or under-representation of 63 GO terms (Fig. 2) and 29 KEGG pathways (Fig. 3), suggesting altered activity of many biochemical and physiological processes in fat body during acclimation. The quantity of differentially-regulated transcripts was similar to that of cold-acclimated *Gryllus pennsylvanicus* tissues (Des Marteaux et al., 2017). Approximately one third (1,054) of the differentially-regulated transcripts had putative gene identities (Dataset S1). Most (2,508) of the differentially-regulated transcripts exhibited different expression patterns between control and acclimated crickets (Fig. 1A, B, D, E, G, and H), and the remaining (800) transcripts changed similarly over time in both conditions (Fig. 1C, F, and I). The latter group of transcripts likely represents changes due to aging, and we therefore focus on the former group to identify transcriptional changes in the fat body that may be important for freeze tolerance. Acclimation likely also initiates differential gene expression in other tissues that may contribute to freeze tolerance, which we have not captured in this experiment.

Most (2,559) of the differentially-expressed transcripts up- or down-regulated at three weeks of acclimation did not change significantly thereafter (Fig. 1A, B, D, E), whereas the remaining transcripts (747) were differentially regulated throughout the six weeks (Fig. 1G, H). However, *G. veletis* only becomes freeze tolerant after six weeks of acclimation (Toxopeus et al., submitted). Therefore, we hypothesize that early differential gene expression (Fig. 1A, B, D, E) contributes to general low temperature tolerance or long-term changes that are necessary for freeze tolerance, e.g. changes to cell structure/function that take several weeks to complete. Additionally, we hypothesize that differential gene expression late in acclimation (Fig. 1G, H) is associated with short-term responses to the freezing process (e.g. mitigating the damaging effects of ice formation). Broadly, we expect both early and late processes to act in synergy to confer freeze tolerance – as well as contribute to general low temperature tolerance – which we expand on in subsequent sections.

How does differential gene expression during acclimation confer freeze tolerance?

Of the five broad mechanisms we hypothesize contribute to freeze tolerance (Toxopeus and Sinclair, 2018), the transcriptional changes in *G. veletis* fat body during acclimation generally support mechanisms 3 (stabilize cells and macromolecules) and 4 (prevent accumulation of

harmful metabolites). For example, acclimated *G. veletis* differentially regulated transcripts involved in membrane lipid biochemistry, cytoskeletal regulation, cryoprotectant transport, and general cytoprotection (Tables 2, 3), which could help stabilize cells at low temperatures and when frozen (Toxopeus and Sinclair, 2018). In addition, *G. veletis* upregulated detoxifying enzymes and downregulated many metabolic enzymes during acclimation (Tables 2, 3), which may contribute to reduced accumulation of harmful metabolic end-products (Toxopeus and Sinclair, 2018). Many of the transcriptional changes parallel those during cold acclimation of chill-susceptible insects, such as differential expression of genes encoding cytoskeletal regulators and antioxidant enzymes in *G. pennsylvanicus* (Des Marteaux et al., 2017) and *Drosophila melanogaster* (MacMillan et al., 2016). We hypothesize that these changes in gene expression increase chill tolerance of *G. veletis*, a requisite for freeze tolerance (Toxopeus and Sinclair, 2018).

Although freeze-tolerant *G. veletis* elevate their SCP and hemolymph osmolality (Toxopeus et al., submitted) – physiological changes that may contribute to mechanisms 1 (control the process of ice formation and propagation) and 2 (reduce ice content), respectively (Toxopeus and Sinclair, 2018) – we did not identify gene expression changes that support these mechanisms. For example, acclimated crickets did not differentially regulate genes required synthesis of low molecular weight cryoprotectants (which could elevate hemolymph osmolality; Table S1). We also did not detect putative ice binding proteins (e.g. INAs that could elevate the SCP) in the transcriptome (Table S2) – that is, the annotation did not identify any putative genes with the GO identifier ‘ice binding,’ or with Pfam domains ‘ice nucleation,’ ‘AFP,’ or ‘CfAFP.’. However, no insect INAs have been sequenced, and ice binding proteins have evolved multiple times (Duman, 2015) which limits our ability to identify putative INAs in freeze-tolerant insects based on homology to known sequences. We identified four putative AQPs in the *G. veletis* transcriptome (Table S1), which may contribute to freeze tolerance by facilitating osmotic dehydration of cells during ice formation (Kikawada et al., 2008; Philip et al., 2008; Li et al., 2009a; Sørensen and Holmstrup, 2013). However, none of these putative AQPs were differentially expressed during acclimation. In the following sections, we elaborate on transcriptional changes in fat body cells that likely support freeze tolerance *via* mechanisms 3 and 4.

Transcriptional regulation of metabolism and cell cycle activity

Acclimated *G. veletis* have slow development and suppressed metabolic rate (Toxopeus et al., submitted), which we expected to see reflected in differential gene expression. *Gryllus veletis* downregulated transcripts in the KEGG pathways 'pentose phosphate pathway,' 'cysteine and methionine metabolism,' 'amino sugar and nucleotide sugar metabolism,' and 'alanine, aspartate and glutamate metabolism' early in acclimation (Figs. 3, S1, Table 3). In addition, acclimated crickets downregulated transcripts with the GO identifiers 'NADH dehydrogenase (ubiquinone) activity,' 'mitochondrial membrane,' and 'respiratory chain' (Fig. 2, Table 3). We hypothesize that these latter changes contribute to downregulation of electron transport activity late in acclimation, similar to dehydrated *Belgica antarctica*, which downregulates several transcripts involved in electron transport and the TCA (tricarboxylic acid) cycle coincident with metabolic rate suppression (Teets et al., 2012a). However, the KEGG pathway 'oxidative phosphorylation' was under-represented in control crickets relative to acclimated crickets (Fig. 3), suggesting that the mechanisms underlying metabolic rate suppression in freeze-tolerant *G. veletis* should be investigated further, particularly given the tentative link between transcription and metabolism (Suarez and Moyes, 2012). In addition, we hypothesize that transcriptional and post-transcriptional changes are required in multiple tissue types to drive whole-animal metabolic rate suppression.

Insects modify metabolism in response to stressors. For example, *B. antarctica* upregulates the genes encoding lipid metabolism enzyme Acyl-CoA dehydrogenase and the rate-limiting enzyme in gluconeogenesis Phophoenolpyruvate kinase (PEPCK) in response to dehydration (Lopez-Martinez et al., 2009; Teets et al., 2012a), while both *B. antarctica* and *Sarcophaga bullata* upregulate *PEPCK* following a cold shock (Teets et al., 2012b; Teets et al., 2013). Aphids starved for 36 h also upregulate both *Acyl-CoA dehydrogenase* and *PEPCK* (Enders et al., 2015). *Gryllus veletis* upregulated transcripts in the 'PPAR signaling pathway' throughout acclimation (Figs. 3, S2), which suggests upregulation of lipid catabolism and carbohydrate metabolism. For example, upregulation of *Medium chain acyl-CoA dehydrogenase* may increase lipid catabolism *via* β-oxidation, and upregulation of *PEPCK* may increase glucose synthesis through the gluconeogenesis pathway (Fig. S2, Table 2). *Gryllus veletis* stops eating late in acclimation and must rely on stored energy reserves. We therefore hypothesize that these transcriptional changes

reflect an increase in lipid consumption (rather than carbohydrates) in response to starvation (Enders et al., 2015; Sinclair et al., 2011). This possible transcriptional restructuring of metabolism may also improve stress tolerance, which we discuss in the next section.

Developmental arrest often accompanies metabolic suppression (Irwin and Lee, 2002): for example, diapausing *C. costata* downregulate genes that promote cell cycle activity and DNA replication (Koštál et al., 2009; Poupardin et al., 2015). We observed some evidence for developmental arrest in the cricket transcriptome. Early in acclimation, *G. veletis* downregulated transcripts with the GO identifier 'positive regulation of cell proliferation' (Fig. 2), and subunits of *DNA polymerase* (Table 3). We therefore hypothesize that *G. veletis* transcriptionally inhibits developmental progression *via* cell cycle arrest during acclimation. Conversely, the KEGG pathways 'DNA replication' and 'cell cycle' were enriched after six weeks of control conditions (Fig. 3). These changes likely promote cell cycle activity and may be an indicator of continued developmental progression under control conditions.

Low molecular weight cryoprotectants and their transporters

Cold-hardy arthropods that accumulate low molecular weight cryoprotectants often upregulate genes encoding cryoprotectant synthesis enzymes, yet we found no evidence of direct transcriptional control of cryoprotectant synthesis in *G. veletis* fat body tissue. *Belgica antarctica* (Teets et al., 2013), *Polypedilum vanderplanki* (Mitsumasu et al., 2010), and *Megaphorura arctica* (Clark et al., 2009) promote trehalose accumulation by upregulating *Trehalose-6-synthase* and/or *Trehalose phosphatase*. Similarly, *D. melanogaster* (MacMillan et al., 2016) and *B. antarctica* (Teets et al., 2012a) upregulate *Pyrroline-5-carboxylate synthase* and/or *reductase* in association with proline accumulation. *Sarcophaga bullata* accumulates *myo*-inositol following cold exposure, concurrent with transcriptional enrichment of the pathways 'inositol phosphate metabolism' and 'glycerolipid metabolism' (Teets et al., 2012b). During acclimation, *G. veletis* did not alter transcript abundance of any cryoprotectant synthesis enzymes (Table S1), and we therefore hypothesize that they post-translationally increase activity of these enzymes (Joanisse and Storey, 1994) to promote cryoprotectant accumulation during acclimation. In addition, we hypothesize that the following transcriptional changes indirectly support cryoprotectant accumulation: 1) *G. veletis* downregulates *Inositol oxygenase* early in acclimation

(Table 3), which may facilitate inositol accumulation by reducing its degradation (Torabinejad and Gillaspy, 2006); 2) transcriptional changes in the 'alanine, aspartate and glutamate metabolism' pathway (Fig. S1) could facilitate the accumulation of glutamate and glutamine, which are precursors for proline synthesis (Weeda et al., 1980); 3) increased gluconeogenesis activity (*via* upregulation of *PEPCK*; Table 2) could increase abundance of glucose, a precursor for the low molecular weight cryoprotectants trehalose (Teets et al., 2012a; Teets et al., 2013) and *myo*-inositol (Loewus and Loewus, 1983).

We expect low molecular weight cryoprotectants to most effectively protect cells when they accumulate intracellularly (Wolkers et al., 2001), a process that likely requires cryoprotectant transmembrane transporters. For example, *P. vanderplanki* (Kikawada et al., 2007) upregulates the *Facilitated trehalose transporter Tret-1* during dehydration, facilitating both trehalose export from fat body, and trehalose import into tissues throughout the insect (Kikawada et al., 2007; Sakurai et al., 2008). This trehalose transporter is not, however, upregulated by chill-susceptible *D. melanogaster* during cold acclimation (MacMillan et al., 2016) or by *B. antarctica* in response to cooling/freezing (Teets et al., 2013). The GO term 'trehalose transport' was enriched in fat body tissue throughout acclimation (Fig. 2), driven by increased transcript abundance of *Tret-1* (Table 2). This study is the first (to our knowledge) to document a correlation between freeze tolerance and the upregulation of a trehalose transporter. We hypothesize that Tret-1 in *G. veletis* facilitates trehalose export from fat body during acclimation, resulting in hemolymph trehalose accumulation. If *Tret-1* is upregulated in other tissues, we hypothesize that this transporter imports trehalose into tissues (Kikawada et al., 2007), facilitating intracellular trehalose accumulation (and therefore cryoprotection) during acclimation and/or freezing (Wolkers et al., 2001). While we detected other putative cryoprotectant transporter genes (i.e. transcripts with GO identifiers 'proline transport' or '*myo*-inositol transport') in the transcriptome (Table S1), *G. veletis* did not differentially express them in fat body tissue. These transporters may instead be post-transcriptionally regulated, or differentially expressed in other tissues.

Upregulation of cytoprotective genes during acclimation

We have previously hypothesized that several families of proteins contribute to macromolecule protection during freezing and thawing, including antioxidants, ion chelators, molecular chaperones, cytochrome P450s (CYPs), disordered proteins, and sirtuins (Toxopeus and Sinclair, 2018). We identified putative genes representing most of these families in the *G. veletis* transcriptome, with the exception of disordered proteins (no annotations containing the words 'disordered' or 'unstructured'; Dataset S1). *Gryllus veletis* upregulated genes putatively encoding one antioxidant, one ion chelator, 13 CYPs, and one molecular chaperone (Table 2, Dataset S1), which may improve chill and freeze tolerance.

Cold-hardy arthropods increase antioxidant capacity to mitigate oxidative stress, and *G. veletis* differentially regulated several transcripts during acclimation that may likewise reduce oxidative damage of macromolecules. For example, many insects upregulate transcription or activity of antioxidant enzymes (e.g. catalase, superoxide dismutase, glutathione S transferase, peroxiredoxins) and CYPs during cold acclimation (Torson et al., 2015; Des Marteaux et al., 2017), in association with freeze tolerance (Joanisse and Storey, 1996; Poupardin et al., 2015), in response to cold shock or freezing (Joanisse and Storey, 1998; Dunning et al., 2014; Štětina et al., 2018), and during or following dehydration (Clark et al., 2009; Lopez-Martinez et al., 2009; Sørensen and Holmstrup, 2013). Freeze-tolerant *E. solidaginis* (Storey and Storey, 2010) and other cold-hardy arthropods (Clark et al., 2009; Rinehart et al., 2010) also upregulate *Ferritin*, which encodes an iron ion chelator that is hypothesized to reduce reactive oxygen species (ROS) production *via* the iron-catalyzed Fenton reaction (Theil, 1987). *Gryllus veletis* upregulated transcripts with GO identifiers related to detoxification (i.e. 'iron ion binding' and 'aromatase activity;' Fig. 2), including *Ferritin* and several putative *CYPs* early in acclimation, and *Catalase* throughout acclimation (Table 2). We hypothesize that the genes upregulated early in acclimation mitigate oxidative stress (e.g. by reducing ROS abundance) during acclimation itself. Because *Catalase* is highly expressed late in acclimation, we hypothesize that accumulation of this antioxidant enzyme protects specifically against oxidative stress associated with freezing and thawing (Doelling et al., 2014).

Many insects upregulate molecular chaperones such as HSPs to mitigate the challenges of thermal stress (King and MacRae, 2015), potentially decreasing protein denaturation and aggregation induced by low temperatures and ice (Rinehart et al., 2006; Toxopeus and Sinclair, 2018). Freeze-tolerant *C. costata* (Poupardin et al., 2015) and *E. solidaginis* (Zhang et al., 2011) upregulate multiple HSP family members (e.g. small HSPs, HSP40, HSP70, HSP83). *Gryllus veletis* upregulated one HSP family member (*HSP70*) early in acclimation (Table 2), but more than 30 other putative heat shock genes were not differentially expressed during acclimation (Table S1). We speculate that *G. veletis* may upregulate additional HSPs, but at different times during acclimation (as in *C. costata*; Poupardin et al., 2015), or in different tissues (as in *Chilo suppressalis*; Lu et al., 2014). Alternatively, *G. veletis* may upregulate cytoprotective proteins after freezing (see Zhang et al., 2011; Lu et al., 2014; Štětina et al., 2018) to facilitate recovery.

Potential cellular remodelling during acclimation

Cold-acclimated insects alter cell membrane composition to retain membrane fluidity at low temperatures (Bennett et al., 1997; Koštál et al., 2011; Koštál et al., 2013), and we observed some transcriptional support for this process in *G. veletis*. Early in acclimation, *G. veletis* upregulated *Stearoyl CoA desaturase* (*SCD*, or *Δ9 fatty acid desaturase*) (Fig. S2, Table 2), a rate-limiting enzyme in synthesis of monounsaturated fatty acids (Stanley-Samuelson et al., 1988). Increased expression of *SCD* is hypothesized to facilitate homeoviscous adaptation of membranes (Clark and Worland, 2008), and is upregulated in cold-tolerant arthropods such as *B. antarctica* (Lopez-Martinez et al., 2009), *C. costata* (Poupardin et al., 2015), *M. arctica* (Sørensen and Holmstrup, 2013), and *Sarcophaga crassipalpis* (Rinehart et al., 2000), but downregulated in hindgut and Malpighian tubules of *G. pennsylvanicus* (Des Marteaux et al., 2017). In addition, *G. veletis* upregulated putative *Acyl transferase* transcripts (Table 2), which could facilitate modification of membrane phospholipid composition (Hazel, 1984). Based on these changes in gene expression, we suggest additional characterization of *G. veletis* to determine whether membrane lipid composition (e.g. Koštál et al., 2003; MacMillan et al., 2009) and fluidity (e.g. Lee et al., 2006) change during acclimation, and the extent to which those changes protect cells at low temperatures and when frozen.

Cold-acclimated or -acclimatized insects can differentially regulate cytoskeletal gene expression (Carrasco et al., 2011; MacMillan et al., 2016; Des Marteaux et al., 2017), which may improve cytoskeleton stability at low temperatures (Kim et al., 2006; Des Marteaux et al., 2018a, b). *Gryllus veletis* differentially-regulated cytoskeletal transcripts, including those with the GO terms 'structural constituent of cytoskeleton' and 'microtubule-based process' during acclimation (Fig. 2). We hypothesize that early differential expression of cytoskeletal genes (e.g. actin-regulators *Supervillin* and *Integrin*; Tables 2, 3) reduces cytoskeletal depolymerization in the cold (see Des Marteaux et al., 2018b), maintaining cell integrity during acclimation. In addition, we hypothesize that differential expression of cytoskeleton genes later in acclimation (e.g. *Actin, alpha-* and *beta-Tubulin*, and *Microtubule-associated protein Jupiter*; Tables 2, 3) are necessary specifically for preserving cell integrity during freezing and thawing.

Regulation of acclimation

We drew inferences from the transcriptome data to identify potential regulation of acclimation at the local (subcellular) or central (neuroendocrine) level. Acclimated *G. veletis* differentially regulated more than 40 transcription factors in fat body tissue (Table S2), and several GO terms related to transcription were enriched throughout acclimation (e.g. 'transcription from RNA polymerase II promoter;' Fig. 2). Similar to acclimated *G. pennsylvanicus* (Des Marteaux et al., 2017), these transcription factors included circadian rhythm regulators such as *Protein cycle* ('circadian regulation of gene expression'; Fig. 2), a transcriptional regulator of the circadian genes *Period* and *Timeless* (Tomioka and Matsumoto, 2010). Our tissue-specific approach identified more transcription factors that might coordinate acclimation than is typical for whole-body transcriptomes (e.g. Poupardin et al., 2015; Torson et al., 2015; MacMillan et al., 2016). However, the downstream effects of most of the differentially-regulated transcription factors are uncharacterized (Table S2). To identify putative downstream targets, we suggest high resolution co-expression or gene network analysis (Alok et al., 2017; Wang et al., 2017; Wang and Chen, 2017; Xing et al., 2017): We predict that transcriptional activators will exhibit similar expression patterns to their targets, while transcriptional repressors will have opposite expression patterns to their targets.

Intracellular signalling is likely an important regulator of gene expression, but we observed few transcriptional changes in cell signalling pathways in *G. veletis* fat body tissue. Cold-acclimated *G. pennsylvanicus* exhibit differential enrichment of more than a dozen KEGG cell signalling pathways in hindgut and Malpighian tubule tissues (Des Marteaux et al., 2017). Conversely, only two KEGG cell signalling pathways were enriched in the fat body of acclimated *G. veletis*: the 'PPAR signaling pathway' and the 'MAPK signaling pathway,' the latter of which was also enriched under control conditions (Figs. 3, S3). Metabolic implications of altered PPAR signalling are discussed above. We hypothesize that slight differences in MAPK signalling between control and acclimated crickets (e.g. downregulation of *Ras GTPase activating protein* in acclimated crickets only; Fig. S3, Table 3) contribute to differences in cell cycle activity and cytoskeletal remodelling (Pearson et al., 2001). MAPK signalling may also alter responses to cold stress (Zhao et al., 2017). We identified several other differentially-regulated transcripts related to signal transduction (Tables 2, 3, S2), but it is challenging to predict the role of these transcriptional changes in cold or freeze tolerance.

Neuroendocrine signalling *via* insulin, JH, and 20HE can coordinate processes such as metabolic regulation and developmental arrest (Denlinger, 2002; Hahn and Denlinger, 2011), and likely influences the acclimation process. For example, several arthropod species differentially regulate genes involved in JH signalling during cold acclimation (Torson et al., 2015; MacMillan et al., 2016; Des Marteaux et al., 2017), and in response to dehydration (Clark et al., 2009; Lopez-Martinez et al., 2009). In addition, freeze-tolerant *C. costata* (Poupardin et al., 2015) and cold-shocked *S. crassipalpis* (Teets et al., 2012b) upregulate ecdysteroid signalling genes. *Gryllus veletis* downregulated an inhibitor of JH signalling, *Juvenile hormone epoxide hydrolase 1* early in acclimation (Table 3), and upregulated transcripts with the GO identifier 'response to insulin' late in acclimation (Fig. 2; Table 2). We did not detect any differential regulation of genes involved in ecdysteroid signalling. Fat body tissue is responsive to both insulin and JH (Sim and Denlinger, 2013), and we hypothesize that these hormones coordinate expression of genes that drive changes in metabolism and developmental progression in *G. veletis* during acclimation (Sim and Denlinger, 2008; Sim and Denlinger, 2013).

Conclusions

Freeze tolerance likely requires coordination of many systems, yet we know little about how insects regulate the changes that promote survival of internal ice formation. By characterizing the transcriptome of the laboratory model *G. veletis*, we generated novel hypotheses about how acclimation promotes freeze tolerance. Specifically, we hypothesize that *G. veletis* also: 1) preserves cell integrity at low temperatures and when frozen by remodelling the cell membrane and cytoskeleton; 2) protects macromolecules by accumulating cryoprotectant transporters, cytoprotective proteins, and antioxidants; and 3) transcriptionally suppresses metabolic and developmental activity (Fig. 4). This broadens our understanding of potential mechanisms that contribute to freeze tolerance, and we encourage further investigation (e.g. by knocking down gene expression with RNA interference) in *G. veletis* and other organisms to test these hypotheses.

Abbreviations

20HE – 20- hydroxyecdysone
AFP – antifreeze protein
AQP – aquaporin
BUSCO – benchmark universal single copy orthologs
CYP – cytochrome P450
FDR – false discovery rate
HSP – heat shock protein
IIF – intracellular ice formation
INA – ice-nucleating agent
JH – juvenile hormone
L:D – light: dark
MAPK – mitogen-activated protein kinase
PEPCK – phosphoenolpyruvate carboxykinase
PFAM – protein family
PPAR – peroxisome proliferator-activated receptor
ROS – reactive oxygen species
RH – relative humidity

SCD – stearoyl CoA dehydrogenase

SCP – supercooling point

TCA – tricarboxylic acid

Acknowledgements

We are grateful to Laura V. Ferguson for assistance with sample preparation, many volunteers for their help with cricket maintenance, and to James F. Staples and two anonymous reviewers for their constructive comments on earlier versions of this manuscript.

Declaration of interest

None. No competing interests declared.

Funding

This work was supported by Discovery Grants from the Natural Sciences and Engineering Research Council of Canada (NSERC) to BJS, and by NSERC Canada Graduate Scholarships and Ontario Graduate Scholarships to JT and LED. These funding bodies played no role in study design; collection, analysis and interpretation of data; writing the manuscript; or in the decision to submit the article for publication.

Data availability

Sequence reads (trimmed) for each library are available in the NCBI Sequence Read Archive (accession no. **SRP151981**). The transcriptome assembly is deposited in the NCBI Transcriptome Shotgun Assembly database (accession no. **GGSD00000000**). The version described in this paper is the first version, **GGSD01000000**. Results of the maSigPro, KEGG, and goseq analyses are available in Dataset S1.

References

Alok, A. K., Saha, S. and Ekbal, A. (2017). Semi-supervised clustering for gene-expression data in multiobjective optimization framework. *Intl. J. Mach. Learning Cybern.* **8**, 421-439.

Altschul, S. F., Gish, W., Miller, W., Myers, E. W. and Lipman, D. J. (1990). Basic local alignment search tool. *J. Mol. Biol.* **215**, 403-410.

Anders, S., Pyl, P. T. and Huber, W. (2015). HTSeq - a Python framework to work with high-throughput sequencing data. *Bioinformatics* **31**, 166-169.

Arrese, E. L. and Soulages, J. L. (2010). Insect fat body: energy, metabolism, and regulation. *Annu. Rev. Entomol.* **55**, 207-225.

Ashburner, M., Ball, C. A., Blake, J. A., Botstein, D., Butler, H., Cherry, J. M., Davis, A. P., Dolinski, K., Dwight, S. S., Eppig, J. T., Harris, M. A., Hill, D. P., Issel-Tarver, L., Kasarskis, A., Lewis, S., Matese, J. C., Richardson, J. E., Ringwald, M., Rubin, G. M. and Sherlock, G. (2000). Gene Ontology: tool for the unification of biology. *Nat. Genet.* **25**, 25-29.

Bayley, J. S., Winther, C. B., Andersen, M. K., Grønkjær, C., Nielsen, O. B., Pedersen, T.H. and Overgaard, J. (2018). Cold exposure causes cell death by depolarization mediated Ca^{2+} overload in a chill-susceptible insect. *Proc. Natl. Acad. Sci. USA* **115**, E9737-E9744.

Bennett, V. A., Pruitt, N. L. and Lee, R. E. (1997). Seasonal changes in fatty acid composition associated with cold-hardening in third instar larvae of *Eurosta solidaginis*. *J. Comp. Physiol. B* **167**, 249-255.

Carrasco, M. A., Buechler, S. A., Arnold, R. J., Sformo, T., Barnes, B. M. and Duman, J. G. (2011). Elucidating the biochemical overwintering adaptations of larval *Cucujus clavipes puniceus*, a nonmodel organism, via high throughput proteomics. *J. Proteome Res.* **10**, 4634-4646.

Clark, M. S., Thorne, M. A. S., Purać, J., Burns, G., Hillyard, G., Popović, Ž. D., Grubor-Lajšić, G. and Worland, M. R. (2009). Surviving the cold: molecular analyses of insect cryoprotective dehydration in the Arctic springtail *Megaphorura arctica* (Tullberg). *BMC Genomics* **10**, 328.

Clark, M. S. and Worland, M. R. (2008). How insects survive the cold: molecular mechanisms - a review. *J. Comp. Physiol. B* **178**, 917-933.

Conesa, A., Nueda, M. J., Ferrer, A. and Talón, M. (2006). maSigPro: a method to identify significantly differential expression profiles in time-course microarray experiments. *Bioinformatics* **22**, 1096-1102.

Courteau, L. A., Storey, K. B. and Morin, P. (2012). Differential expression of microRNA species in a freeze tolerant insect, *Eurosta solidaginis*. *Cryobiology* **65**, 210-214.

Denlinger, D. L. (2002). Regulation of diapause. *Annu. Rev. Entomol.* **47**, 93-122.

Dennis, A. B., Dunning, L. T., Sinclair, B. J. and Buckley, T. R. (2015). Parallel molecular routes to cold adaptation in eight genera of New Zealand stick insects. *Sci. Rep.* **5**, 13965.

Des Marteaux, L. E., McKinnon, A. H, Udaka, H., Toxopeus, J. and Sinclair, B. J. (2017). Effects of cold-acclimation on gene expression in Fall field cricket (*Gryllus pennsylvanicus*) ionoregulatory tissues. *BMC Genomics* **18**, 357.

Des Marteaux, L. E., Štětina, T. and Koštál, V. (2018a). Insect fat body cell morphology and response to cold stress is modulated by acclimation. *J. Exp. Biol.* doi:

10.1242/jeb.189647.

Des Marteaux, L. E., Stinziano, J. R. and Sinclair, B. J. (2018b). Effects of cold acclimation on rectal macromorphology, ultrastructure, and cytoskeletal stability in *Gryllus pennsylvanicus* crickets. *J. Insect Physiol.* **104**, 15-24.

Dias, C. L., Ala-Nissila, T., Wong-ekkabut, J., Vattulainen, I., Grant, M. and Karttunen, M. (2010). The hydrophobic effect and its role in cold denaturation. *Cryobiology* **60**, 91-99.

Doelling, A. R., Griffis, N. and Williams, J. B. (2014). Repeated freezing induces oxidative stress and reduces survival in the freeze-tolerant goldenrod gall fly, *Eurosta solidaginis*. *J. Insect Physiol.* **67**, 20-27.

Duman, J. G. (2015). Animal ice-binding (antifreeze) proteins and glycolipids: an overview with emphasis on physiological function. *J. Exp. Biol.* **218**, 1846-1855.

Dunning, L. T., Dennis, A. B., Sinclair, B. J., Newcomb, R. D. and Buckley, T. R. (2014). Divergent transcriptional responses to low temperature among populations of alpine and lowland species of New Zealand stick insects (*Micrarchus*). *Mol. Ecol.* **23**, 2712-2726.

Enders, L. S., Bickel, R. D., Brisson, J. A., Heng-Moss, T. M., Siegfried, B. D., Zera, A. J. and Miller, N. J. (2015). Abiotic and biotic stressors causing equivalent mortality induce highly variable transcriptional responses in the soybean aphid. *Genes, Genomes, Genetics* **5**, 261-270.

Grabherr, M. G., Haas, B. J., Yassour, M., Levin, J. Z., Thompson, D. A., Amit, I., Adiconis, X., Fan, L., Raychowdhury, R., Zeng, Q., Chen, Z., Mauceli, E., Hacohen, N., Gnirke, A., Rhind, N., di Palma, F., Birren, B. W., Nusbaum, C., Lindblad-Toh, K., Friedman, N. and Regev, A. (2011). Full-length transcriptome assembly from RNA-Seq data without a reference genome. *Nat. Biotech.* **29**, 644-652.

Haas, B. J., Papanicolaou, A., Yassour, M., Grabherr, M., Blood, P. D., Bowden, J., Couger, M. B., Eccles, D., Li, B., Lieber, M., MacManes, M. D., Ott, M., Orvis, J., Pochet, N., Strozzi, F., Weeks, N., Westerman, R., William, T., Dewey, C. N., Henschel, R., LeDuc, R. D., Friedman, N. and Regev, A. (2013). De novo transcript sequence reconstruction from RNA-seq using the Trinity platform for reference generation and analysis. *Nat. Protocols* **8**, 1494-1512.

Hahn, D. A. and Denlinger, D. L. (2011). Energetics of insect diapause. *Annu. Rev. Entomol.* **56**, 103-121.

Hazel, J. R. (1984). Effects of temperature on the structure and metabolism of cell membranes in fish. *Am. J. Physiol.* **246**, R460-R470.

Hazel, J. R. (1995). Thermal adaptation in biological membranes: is homeoviscous adaptation the explanation? *Annu. Rev. Physiol.* **57**, 19-42.

Irwin, J. T. and Lee, R. E. (2002). Energy and water conservation in frozen vs. supercooled larvae of the goldenrod gall fly, *Eurosta solidaginis* (Fitch) (Diptera: Tephritidae). *J. Exp. Zool.* **292**, 345-350.

Joanisse, D. R. and Storey, K. B. (1994). Enzyme activity profiles in an overwintering population of freeze-tolerant larvae of the gall fly, *Eurosta solidaginis*. *J. Comp. Physiol. B* **164**, 247-255.

Joanisse, D. R. and Storey, K. B. (1996). Oxidative stress and antioxidants in overwintering larvae of cold-hardy goldenrod gall insects. *J. Exp. Biol.* **199**, 1483-1491.

Joanisse, D. R. and Storey, K. B. (1998). Oxidative stress and antioxidants in stress and recovery of cold-hardy insects. *Insect Biochem. Mol. Biol.* **28**, 23-30.

Kanehisa, M., Goto, S., Sato, Y., Furumichi, M. and Tanabe, M. (2011). KEGG for integration and interpretation of large-scale molecular data sets. *Nucleic Acids Res.* **40**, D109-D114.

Kikawada, T., Saito, A., Kanamori, Y., Fujita, M., Śnigórska, K., Watanabe, M. and Okuda, T. (2008). Dehydration-inducible changes in expression of two aquaporins in the sleeping chironomid, *Polypedilum vanderplanki*. *Biochimica Biophysica Acta* **1778**, 514-520.

Kikawada, T., Saito, A., Kanamori, Y., Nakahara, Y., Iwata, K.-i., Tanaka, D., Watanabe, M. and Okuda, T. (2007). Trehalose transporter 1, a facilitated and high-capacity trehalose transporter, allows exogenous trehalose uptake into cells. *Proc. Natl. Acad. Sci. USA* **104**, 11585-11590.

Kim, M., Robich, R. M., Rinehart, J. P. and Denlinger, D. L. (2006). Upregulation of two actin genes and redistribution of actin during diapause and cold stress in the northern house mosquito, *Culex pipiens*. *J. Insect Physiol.* **52**, 1226-1233.

King, A. M. and MacRae, T. H. (2015). Insect heat shock proteins during stress and diapause. *Annu. Rev. Entomol.* **60**, 59-75.

Koštál, V., Berková, P. and Šimek, P. (2003). Remodelling of membrane phospholipids during transition to diapause and cold-acclimation in the larvae of *Chymomyza costata* (Drosophilidae). *Comp. Biochem. Physiol. B* **135**, 407-419.

Koštál, V., Korbelová, J., Rozsypal, J., Zahradníčková, H., Cimlová, J., Tomčala, A. and Šimek, P. (2011). Long-term cold acclimation extends survival time at 0°C and modifies the metabolomic profiles of the larvae of the fruit fly *Drosophila melanogaster*. *PLoS One* **6**, e25025.

Koštál, V., Šimůnková, P., Kobelková, A. and Shimada, K. (2009). Cell cycle arrest as a hallmark of insect diapause: changes in gene transcription during diapause induction in the drosophilid fly, *Chymomyza costata*. *Insect Biochem. Mol. Biol.* **39**, 875-883.

Koštál, V., Štětina, T., Poupardin, R., Korbelová, J. and Bruce, A. W. (2017). Conceptual framework of the eco-physiological phases of insect diapause development justified by transcriptomic profiling. *Proc. Natl. Acad. Sci. USA* **114**, 8532-8537.

Koštál, V., Urban, T., Řimnáčová, L., Berková, P. and Šimek, P. (2013). Seasonal changes in minor membrane phospholipid classes, sterols and tocopherols in overwintering insect, *Pyrrhocoris apterus*. *J. Insect Physiol.* **59**, 934-941.

Lalouette, L., Williams, C., Hervant, F., Sinclair, B. J. and Renault, D. (2011). Metabolic rate and oxidative stress in insects exposed to low temperature thermal fluctuations. *Comp. Biochem. Physiol. A* **158**, 229-234.

Langmead, B. and Salzberg, S. L. (2012). Fast gapped-read alignment with Bowtie 2. *Nat. Methods* **9**, 357-359.

Lee, R. E. (2010). A primer on insect cold-tolerance. In: Denlinger, D. L. and Lee, R. E. (Eds.) *Low Temperature Biology of Insects*. Cambridge University Press, New York, pp. 3-34.

Lee, R. E., Damodaran, K., Yi, S.-X. and Lorigan, G. A. (2006). Rapid cold-hardening increases membrane fluidity and cold tolerance of insect cells. *Cryobiology* **52**, 459-463.

Li, A., Benoit, J. B., Lopez-Martinez, G., Elnitsky, M. A., Lee, R. E. and Denlinger, D. L. (2009a). Distinct contractile and cytoskeletal protein patterns in the Antarctic midge are elicited by desiccation and rehydration. *Proteomics* **9**, 2788-2798.

Li, H., Handsaker, B., Wysoker, A., Fennell, T., Ruan, J., Homer, N., Marth, G., Abecasis, G. and Durbin, R. (2009b). The sequence alignment/map format and SAMtools. *Bioinformatics* **25**, 2078-2079.

Loewus, F. A. and Loewus, M. W. (1983). *Myo*-inositol: its biosynthesis and metabolism. *Annu. Rev. Plant Physiol.* **34**, 137-161.

Lopez-Martinez, G., Benoit, J. B., Rinehart, J. P., Elnitsky, M. A., Lee, R. E. and Denlinger, D. L. (2009). Dehydration, rehydration, and overhydration alter patterns of gene expression in the Antarctic midge, *Belgica antarctica*. *J. Comp. Physiol. B* **179**, 481-491.

Lu, M.-X., Liu, Z.-X., Cui, Y.-D. and Du, Y.-Z. (2014). Expression patterns of three heat shock proteins in *Chilo suppressalis* (Lepidoptera: Pyralidae). *Annu. Entomol. Soc. Am.* **107**, 667-673.

Luo, W. and Brouwer, C. (2013). Pathview: an R/Bioconductor package for pathway-based data integration and visualization. *Bioinformatics* **29**, 1830-1831.

Luo, W., Friedman, M. S., Shedden, K., Hankenson, K. D. and Woolf, P. J. (2009). GAGE: generally applicable gene set enrichment for pathway analysis. *BMC Bioinform.* **10**, 161.

MacMillan, H. A., Guglielmo, C. G. and Sinclair, B. J. (2009). Membrane remodeling and glucose in *Drosophila melanogaster*: a test of rapid cold-hardening and chilling tolerance hypotheses. *J. Insect Physiol.* **55**, 243-249.

MacMillan, H. A., Knee, J. M., Dennis, A. B., Udaka, H., Marshall, K. E., Merritt, T. J. and Sinclair, B. J. (2016). Cold acclimation wholly reorganizes the *Drosophila melanogaster* transcriptome and metabolome. *Sci. Rep.* **6**, 28999.

Martin, M. (2011). Cutadapt removes adapter sequences from high-throughput sequencing reads. *EMBnet J.* **17**, 10-12.

Mitsumasu, K., Kanamori, Y., Fujita, M., Iwata, K. i., Tanaka, D., Kikuta, S., Watanabe, M., Cornette, R., Okuda, T. and Kikawada, T. (2010). Enzymatic control of anhydrobiosis-related accumulation of trehalose in the sleeping chironomid, *Polypedilum vanderplanki*. *FEBS J.* **277**, 4215-4228.

Pearson, G., Robinson, F., Beers Gibson, T., Xu, B., Karandikar, M., Berman, K. and Cobb, M. H. (2001). Mitogen-activated protein (MAP) kinase pathways: regulation and physiological functions. *Endocr. Rev.* **22**, 153-183.

Pegg, D. E. (2010). The relevance of ice crystal formation for the cryopreservation of tissues and organs. *Cryobiology* **60**, S36-44.

Philip, B. N. and Lee, R. E. (2010). Changes in abundance of aquaporin-like proteins occurs concomitantly with seasonal acquisition of freeze tolerance in the goldenrod gall fly, *Eurosta solidaginis*. *J. Insect Physiol.* **56**, 679–685.

Philip, B. N., Yi, S.-X., Elnitsky, M. A. and Lee, R. E. (2008). Aquaporins play a role in desiccation and freeze tolerance in larvae of the goldenrod gall fly, *Eurosta solidaginis*. *J. Exp. Biol.* **211**, 1114-1119.

Poupardin, R., Schöttner, K., Korbelová, J., Provazník, J., Doležel, D., Pavlinic, D., Beneš, V. and Koštál, V. (2015). Early transcriptional events linked to induction of diapause revealed by RNAseq in larvae of drosophilid fly, *Chymomyza costata*. *BMC Genomics* **16**, 720.

Punta, M., Coggill, P. C., Eberhardt, R. Y., Mistry, J., Tate, J., Boursnell, C., Pang, N., Forslund, K., Ceric, G., Clements, J., Heger, A., Holm, L., Sonnhammer, E. L. L., Eddy, S. R., Bateman, A. and Finn, R. D. (2011). The Pfam protein families database. *Nucleic Acids Res.* **40**, D290-D301.

R Core Team. (2017). R: A Language and Environment for Statistical Computing. R Foundation for Statistical Computing, Vienna.

Rinehart, J. P., Hayward, S. A. L., Elnitsky, M. A., Sandro, L. H., Lee, R. E. and Denlinger, D. L. (2006). Continuous up-regulation of heat shock proteins in larvae, but not adults, of a polar insect. *Proc. Natl. Acad. Sci. USA* **103**, 14223-14227.

Rinehart, J. P., Robich, R. M. and Denlinger, D. L. (2010). Isolation of diapause-regulated genes from the flesh fly, *Sarcophaga crassipalpis* by suppressive subtractive hybridization. *J. Insect Physiol.* **56**, 603-609.

Rinehart, J. P., Yocum, G. D. and Denlinger, D. L. (2000). Developmental upregulation of inducible hsp70 transcripts, but not the cognate form, during pupal diapause in the flesh fly, *Sarcophaga crassipalpis*. *Insect Biochem. Mol. Biol.* **30**, 515-521.

Risso, D., Ngai, J., Speed, T. P. and Dudoit, S. (2014). Normalization of RNA-seq data using factor analysis of control genes or samples. *Nat. Biotech.* **32**, 896-902.

Robinson, M. D., McCarthy, D. J. and Smyth, G. K. (2010). edgeR: a Bioconductor package for differential expression analysis of digital gene expression data. *Bioinformatics* **26**, 139-140.

Sakurai, M., Furuki, T., Akao, K.-i., Tanaka, D., Nakahara, Y., Kikawada, T., Watanabe, M. and Okuda, T. (2008). Vitrification is essential for anhydrobiosis in an African chironomid, *Polypedilum vanderplanki*. *Proc. Natl. Acad. Sci. USA* **105**, 5093-5098.

Sim, C. and Denlinger, D. L. (2008). Insulin signaling and FOXO regulate the overwintering diapause of the mosquito *Culex pipiens*. *Proc. Natl. Acad. Sci. USA* **105**, 6777-6781.

Sim, C. and Denlinger, D. L. (2013). Juvenile hormone III suppresses forkhead of transcription factor in the fat body and reduces fat accumulation in the diapausing mosquito, *Culex pipiens*. *Insect Mol. Biol.* **22**, 1-11.

Simão, F. A., Waterhouse, R. M., Ioannidis, P., Kriventseva, E. V. and Zdobnov, E. M. (2015). BUSCO: assessing genome assembly and annotation completeness with single-copy orthologs. *Bioinformatics*, btv351.

Sinclair, B. J., Bretman, A., Tregenza, T., Tomkins, J. L. and Hosken, D. J. (2011). Metabolic rate does not decrease with starvation in *Gryllus bimaculatus* when changing fuel use is taken into account. *Physiol. Entomol.* **36**, 84-89.

Sinclair, B. J. and Marshall, K. E. (2018). The many roles of fats in overwintering insects. *J. Exp. Biol.* **221**, doi: 10.1242/jeb.161836.

Sørensen, J. G. and Holmstrup, M. (2013). Candidate gene expression associated with geographical variation in cryoprotective dehydration of *Megaphorura arctica*. *J. Insect Physiol.* **59**, 804-811.

Stanley-Samuelson, D. W., Jurenka, R. A., Cripps, C., Blomquist, G. J. and de Renobales, M. (1988). Fatty acids in insects: composition, metabolism, and biological significance. *Archives Insect Biochem. Physiol.***9**, 1-33.

Štětina, T., Hůla, P., Moos, M., Šimek, P., Šmilauer, P. and Koštál, V. (2018). Recovery from supercooling, freezing, and cryopreservation stress in larvae of the drosophilid fly, *Chymomyza costata*. *Sci. Rep.* **8**, 4414.

Storey, J. M. and Storey, K. B. (1985). Freezing and cellular metabolism in the gall fly larva, *Eurosta solidaginis*. *J. Comp. Physiol. B* **155**, 333-337.

Storey, K. B. and Storey, J. M. (1981). Biochemical strategies of overwintering in the gall fly larva, *Eurosta solidaginis*: effect of low temperature acclimation on the activities of enzymes of intermediary metabolism. *J. Comp. Physiol. B* **144**, 191-199.

Storey, K. B. and Storey, J. M. (2010). Oxygen: stress and adaptation in cold hardy insects. In: Denlinger, D. L. and Lee, R. E. (Eds.) *Low Temperature Biology of Insects*. Cambridge University Press, New York, pp. 141-165.

Suarez, R. K. and Moyes, C. D. (2012). Metabolism in the age of 'omes'. *J. Exp. Biol.* **215**, 2351-2357.

Supek, F., Bošnjak, M., Škunca, N. and Šmuc, T. (2011). REViGO summarizes and visualizes long lists of gene ontology terms. *PLoS One* **6**, e21800.

Tassone, E. E., Geib, S. M., Hall, B., Fabrick, J. A., Brent, C. S. and Hull, J. J. (2016). *De novo* construction of an expanded transcriptome assembly for the western tarnished plant bug, *Lygus hesperus*. *GigaScience* **5**, 6.

Teets, N. M., Kawarasaki, Y., Lee, R. E. and Denlinger, D. L. (2013). Expression of genes involved in energy mobilization and osmoprotectant synthesis during thermal and dehydration stress in the Antarctic midge, *Belgica antarctica*. *J. Comp. Physiol. B* **183**, 189-201.

Teets, N. M., Peyton, J. T., Colinet, H., Renault, D., Kelley, J. L., Kawarasaki, Y., Lee, R. E. and Denlinger, D. L. (2012a). Gene expression changes governing extreme dehydration tolerance in an Antarctic insect. *Proc. Natl. Acad. Sci. USA* **109**, 20744-20749.

Teets, N. M., Peyton, J. T., Ragland, G. J., Colinet, H., Renault, D., Hahn, D. A. and Denlinger, D. L. (2012b). Combined transcriptomic and metabolomic approach uncovers molecular mechanisms of cold tolerance in a temperate flesh fly. *Physiol. Genomics* **44**, 764-777.

Theil, E. C. (1987). Ferritin: structure, gene regulation, and cellular function in animals, plants, and microorganisms. *Annu. Rev. Biochem.* **56**, 289-315.

Theissinger, K., Falckenhayn, C., Blande, D., Toljamo, A., Gutekunst, J., Makkonen, J., Jussila, J., Lyko, F., Schrimpf, A. and Schulz, R. (2016). *De novo* assembly and annotation of the freshwater crayfish *Astacus astacus* transcriptome. *Marine Genomics* **28**, 7-10.

Tomioka, K. and Matsumoto, A. (2010). A comparative view of insect circadian clock systems. *Cell Mol. Life Sci.* **67**, 1397-1406.

Torabinejad, J. and Gillaspy, G. E. (2006). Functional genomics of inositol metabolism. In Lahiri Majumder, A. and Biswas, B. B. (Eds.) *Biology of Inositols and Phosphoinositides*. Springer, Amsterdam, pp. 47-70.

Torson, A. S., Yocum, G. D., Rinehart, J. P., Kemp, W. P. and Bowsher, J. H. (2015). Transcriptional responses to fluctuating thermal regimes underpinning differences in survival in the solitary bee *Megachile rotundata*. *J. Exp. Biol.* **218**, 1060-1068.

Toxopeus, J. and Sinclair, B.J. (2018). Mechanisms underlying insect freeze tolerance. *Biol. Rev.* doi: 10.1111/brv.12425.

Toxopeus, J., McKinnon, A.H, Štětina, T., Turnbull, K.F., and Sinclair, B.J. (submitted). Laboratory acclimation to autumn-lke conditions induces freeze tolerance in the spring field cricket *Gryllus veletis* (Orthoptera: Gryllidae).

Trapnell, C., Roberts, A., Goff, L., Pertea, G., Kim, D., Kelley, D. R., Pimentel, H., Salzberg, S. L., Rinn, J. L. and Pachter, L. (2012). Differential gene and transcript expression analysis of RNA-seq experiments with TopHat and Cufflinks. *Nat. Protocols* **7**, 562-578.

Wang, L., Ahsan, M. A. and Chen, M. (2017). A generalized approach for measuring relationships among genes. *J. Integr. Bioinform.* **14**.

Wang, Q. and Chen, G. (2017). Fuzzy soft subspace clustering method for gene co-expression network analysis. *Intl. J. Mach. Learning Cybern.* **8**, 1157-1165.

Weeda, E., Koopmanschap, A., De Kort, C. and Beenakkers, A. T. (1980). Proline synthesis in fat body of *Leptinotarsa decemlineata*. *Insect Biochem.* **10**, 631-636.

Wolkers, W. F., Walker, N. J., Tablin, F. and Crowe, J. H. (2001). Human platelets loaded with trehalose survive freeze-drying. *Cryobiology* **42**, 79-87.

Xing, L., Guo, M., Liu, X., Wang, C., Wang, L. and Zhang, Y. (2017). An improved Bayesian network method for reconstructing gene regulatory network based on candidate auto selection. *BMC Genomics* **18**, 844.

Yi, S.-X., Benoit, J. B., Elnitsky, M. A., Kaufmann, N., Brodsky, J. L., Zeidel, M. L., Denlinger, D. L. and Lee, R. E. (2011). Function and immuno-localization of aquaporins in the Antarctic midge *Belgica antarctica*. *J. Insect Physiol.* **57**, 1096-1105.

Young, M. D., Wakefield, M. J., Smyth, G. K. and Oshlack, A. (2010). Gene ontology analysis for RNA-seq: accounting for selection bias. *Genome Biol.* **11**, R14.

Zachariassen, K. E., Kristiansen, E., Pedersen, S. A. and Hammel, H. T. (2004). Ice nucleation in solutions and freeze-avoiding insects-homogeneous or heterogeneous? *Cryobiology* **48**, 309-321.

Zhang, G., Storey, J. M. and Storey, K. B. (2011). Chaperone proteins and winter survival by a freeze tolerant insect. *J. Insect Physiol.* **57**, 1115-1122.

Zhao, C., Wang, P., Si, T., Hsu, C .C., Wang, L., Zayed, O., Yu, Z., Zhu, Y., Dong, J., Tao, W.A. and Zhu, J. K. (2017). MAP kinase cascades regulate the cold response by modulating ICE1 protein stability. *Develop. Cell* **43**, 618-629.

Figure legends

Figure 1 – Acclimation alters patterns of gene expression in *Gryllus veletis* fat body. Transcripts were clustered into expression profiles using the maSigPro package for R. Each line indicates relative median expression (arbitrary units) of three biological replicates at each time point under control (red, solid line) or acclimation (blue, dashed line) conditions. Each panel represents for one cluster of transcripts that share a common expression pattern, with the number of transcripts in that cluster indicated above the panel. Dots represent outliers, with each dot representing one putative transcript. The list of transcripts in each cluster is available in Dataset S1.

Figure 2 – Relative enrichment of GO terms in *Gryllus veletis* fat body during six weeks in control or acclimation conditions. Differentially-expressed GO categories in each group of crickets (at three and six weeks of control or acclimation conditions) relative to the zero-week control (FDR-corrected $P < 0.1$), based on three biological replicates at each time point. The number of transcripts in each GO category that are represented in the *G. veletis* transcriptome is indicated in parentheses. The circle area represents the relative proportion (0 to 100 %; relative sizes indicated in the legend, bottom right) of transcripts within each GO category that was upregulated (filled) or downregulated (open) in the treatment group

Figure 3 – Summary of KEGG pathway enrichment in *Gryllus veletis* fat body during six weeks in control or acclimation conditions. Each box represents the enrichment of transcripts in a KEGG pathway in one biological replicate (1, 2, or 3) within a treatment group (three and six weeks of control or acclimation conditions) relative to the average expression in the zero-week control (FDR-corrected $P < 0.1$). Blue indicates over-representation (positive GAGE statistic) and yellow indicates under-representation (negative GAGE statistic) of a KEGG pathway; solid grey areas indicate that transcript abundance in that pathway did not differ from zero-week controls. Selected KEGG pathway diagrams are available in Figs. S1-3.

Figure 4 – Candidate mechanisms of freeze tolerance acclimation in *Gryllus veletis* fat body tissue. Processes associated with acclimation that are hypothesized to preserve cell structure, protect macromolecules, and reduce metabolic and developmental activity. Changes in transcript

abundancer that support each process are listed under the arrows. Straight arrows indicate transcript expression that changes early and then plateaus; widening arrows indicate transcript expression that changes throughout acclimation. The predicted effect of each process is described under each cell icon. CYP, cytochrome P450; HSP70, heat shock protein 70.

Tables

Table 1. Summary of the *Gryllus veletis* transcriptome *de novo* assembly. bp, base pairs; GC %, percentage of transcriptome comprised of guanines and cytosines; N50, weighted median statistic.

Sequencing & Quality Control	
Libraries	16
125-bp paired-end reads (raw)	672,647,607
125-bp paired-end reads (trimmed/cleaned)	666,449,419
Trinity Assembly	
Assembly length (bp)	108,582,884
Contigs	136,332
Mean contig length (bp)	796
Median contig length (bp)	396
N50	1429
GC %	40
BUSCO Analysis[a]	
Complete BUSCOs	77.6 %
Fragmented BUSCOs	5.5 %
Missing BUSCOs	16.9 %
Trinotate Annotation	
Contigs with BLAST hit	27,311
Contigs with GO description	24,688
Contigs with KEGG IDs	13,308
Contigs with Pfam domain(s)	18,331

[a]Percentage of the 2,675 Arthropod BUSCOs (Benchmark Universal Single Copy Orthologs) in the transcriptome assembly.

Table 2. Selected transcripts upregulated in *Gryllus veletis* during acclimation whose putative function in freeze tolerance is discussed in the text. Pattern refers to the maSigPro clusters; i.e. the panels in Fig. 1. Select KEGG pathways are illustrated in Figs S1-3. Fold change indicates the $\log_2$(fold change), calculated in edgeR relative to zero-week control crickets.

					Fold change	
Function	Description	Contig ID	Pattern	KEGG	3 wk	6 wk
Metabolism						
Gluconeogenesis	Glycerol kinase	Gvel_56057_c0_g1_i2	D	ko03320	2.19	2.41
	Phosphoenolpyruvate carboxykinase (PEPCK)	Gvel_47855_c0_g2_i1		ko03320	2.37	2.41
	6-Phosphofructo-2-kinase/Fructose-2,6-bisphosphatase	Gvel_54367_c0_g1_i1	E		2.72	2.34
Lipid metabolism	Medium chain acyl-CoA dehydrogenase	Gvel_18079_c0_g1_i1		ko03320	2.73	1.96
	Stearoyl CoA desaturase	Gvel_67809_c0_g1_i1	E	ko03320	1.79	2.05
	1-acyl-sn-glycerol-3-phosphate acyltransferase	Gvel_62590_c2_g1_i1	E		2.53	2.40
Transport						
Trehalose transport	Facilitated trehalose transporter Tret-1	Gvel_80068_c0_g1_i1	E		3.28	3.57
		Gvel_51736_c0_g2_i2	H		3.79	5.12
Cytoskeleton proteins and regulators						
Microtubules	Tubulin (alpha)	Gvel_16545_c0_g1_i1	H		1.33	1.58
		Gvel_8000_c0_g1_i1	E		1.98	1.99
	Tubulin (beta)	Gvel_43107_c1_g1_i1	H		2.31	2.76
Myosin regulators	Microtubule-associated protein Jupiter	Gvel_79158_c0_g1_i2	G		1.75	3.67
Actin regulators	Supervillin	Gvel_64991_c0_g1_i1	E		2.51	2.36
Cell protection						
Detoxification	Cytochrome P450 4C1	Gvel_10729_c0_g1_i1	E		4.86	4.62
	Cytochrome P450 6a23	Gvel_69868_c0_g1_i1	E		4.61	3.74
	Cytochrome P450 6k1	Gvel_10560_c0_g3_i5	E		4.81	3.72
	Cytochrome P450 6j1	Gvel_39812_c2_g1_i1	E		4.19	4.69
Chaperones	Heat shock protein 70	Gvel_60996_c0_g1_i2	D		1.36	1.16
Antioxidants	Catalase	Gvel_66513_c3_g1_i1	H	ko04146	1.02	2.11
	Ferritin heavy chain	Gvel_62685_c1_g2_i1	E		2.79	3.16
Cellular processes						
Transcription	RNA polymerases I, II, and III subunit RPACBC3	Gvel_16630_c0_g2_i1	E		3.74	3.61
Cell cycle & division	Death-associated inhibitor of apoptosis 1	Gvel_56478_c0_g1_i1	D		0.96	0.62
Signal transduction						
AMP kinase pathway	5'-AMP-activated protein kinase subunit gamma-2	Gvel_61474_c0_g1_i1	E		1.40	1.65
cAMP pathways	Adenylate cyclase type 5	Gvel_28980_c0_g4_i4	D		3.00	2.60
	G-protein coupled receptor Mth	Gvel_35842_c0_g1_i1	H		1.82	2.38
	G-protein coupled receptor Mth2	Gvel_27887_c0_g1_i1	E		2.91	2.23
Endocrine						
Insulin signalling	Insulin-like peptide receptor	Gvel_33468_c0_g1_i1	H		2.23	2.34

Table 3. Selected transcripts downregulated in *Gryllus veletis* during acclimation whose putative function in freeze tolerance is discussed in the text. Pattern refers to the maSigPro clusters; i.e. the panels in Fig. 1. Select KEGG pathways are illustrated in Figs S1-3. Fold change indicates the $\log_2$(fold change), calculated in edgeR relative to zero-week control crickets.

					Fold change	
Function	Description	Contig ID	Pattern	KEGG	3 wk	6 wk
Metabolism						
Pentose phosphate pathway	Gluconolactonase	Gvel_9398_c0_g2_i1	A	ko00030	2.00	2.38
Tricarboxylic acid (TCA) cycle	Isocitrate dehydrogenase subunit gamma	Gvel_54615_c0_g1_i1	A		1.99	0.72
Electron transport system	NADH-ubiquinone oxidoreductase chain 1	Gvel_44854_c1_g1_i1	C		0.39	1.31
	NADH-ubiquinone oxidoreductase chain 3	Gvel_46034_c0_g1_i1	C		0.59	1.99
	NADH-ubiquinone oxidoreductase chain 5	Gvel_41420_c0_g1_i1	C		1.34	2.65
Amino acid metabolism	Alanine-glyoxylate transaminase	Gvel_56575_c0_g1_i1	A	ko04146	2.68	2.79
	Alanine aminotransferase	Gvel_31546_c0_g1_i1	A		1.20	1.66
Polyol metabolism	Inositol oxygenase	Gvel_26533_c0_g3_i4			2.65	1.51
Cytoskeleton proteins and regulators						
Microfilament	Actin	Gvel_18303_c0_g1_i1			0.89	1.56
Actin regulators	Integrin	Gvel_32105_c2_g1_i1	A		1.40	1.38
Cellular processes						
DNA replication	DNA polymerase alpha catalytic subunit	Gvel_31138_c0_g1_i1		ko03030	1.48	1.47
	DNA polymerase delta catalytic subunit	Gvel_11665_c0_g1_i1		ko03030	1.65	1.62
Cell cycle & division	Serine/threonine-protein kinase Chk2	Gvel_15060_c0_g1_i1	B		2.67	3.08
	Caspase-1	Gvel_79011_c0_g1_i2	A		1.55	1.77
Signal transduction						
MAPK pathway	Ras GTPase activating protein 1	Gvel_17341_c0_g1_i2	B	ko04013	1.03	1.22
Phosphatidylinositol pathway	Inositol 1,4,5-trisphosphate receptor	Gvel_41178_c0_g4_i1	B		1.62	1.76
	Phosphatidylinositol 5-phosphate 4-kinase	Gvel_53190_c0_g1_i1	B		1.08	1.09
	Phosphatidylinositol phosphatase PTPRQ	Gvel_80174_c5_g1_i1	A		1.43	1.59
Endocrine						
Juvenile hormone signalling	Juvenile hormone epoxide hydrolase 1	Gvel_46923_c0_g1_i1	B		0.86	1.33

Figures

Figure 1

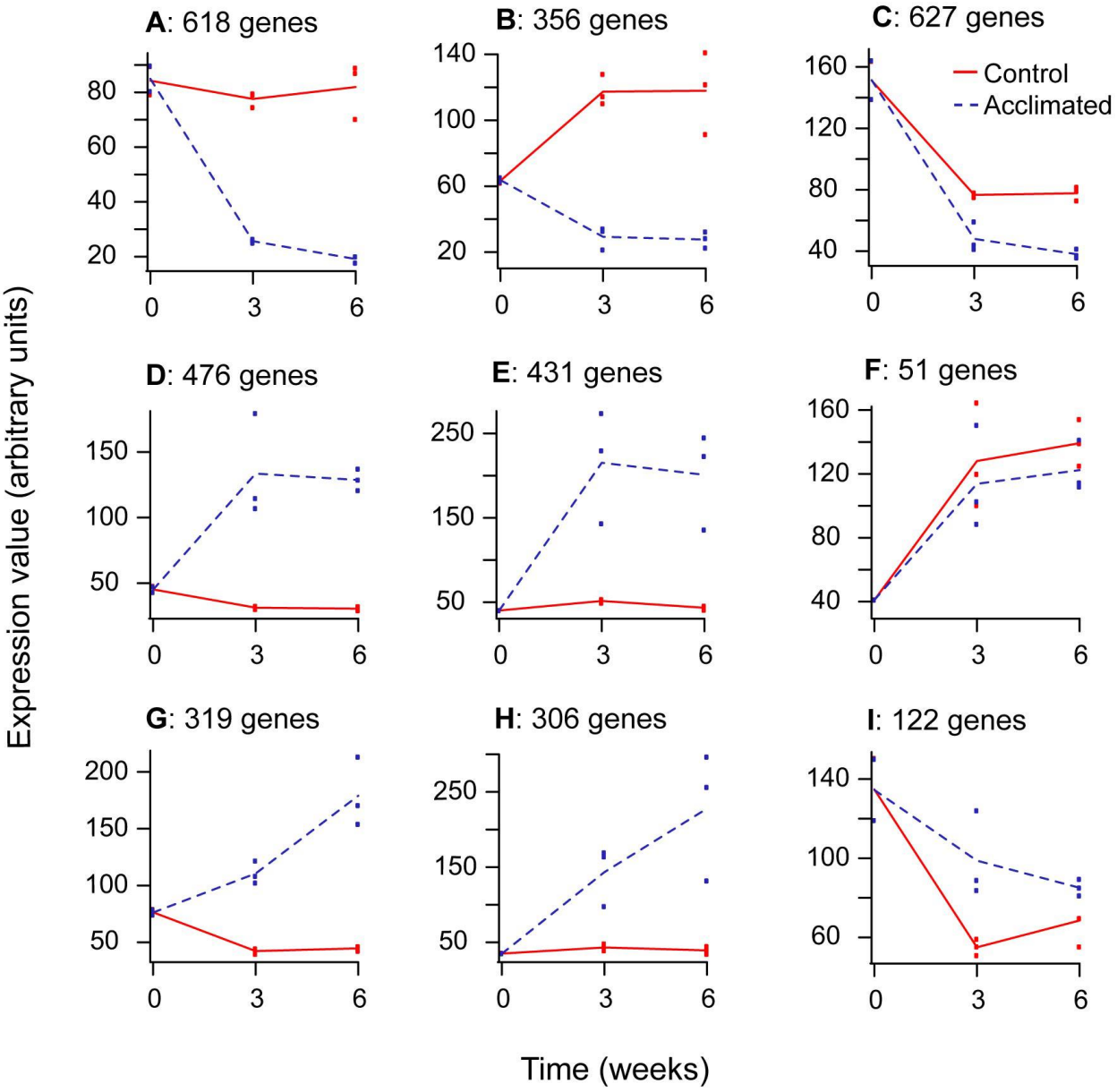

Figure 2

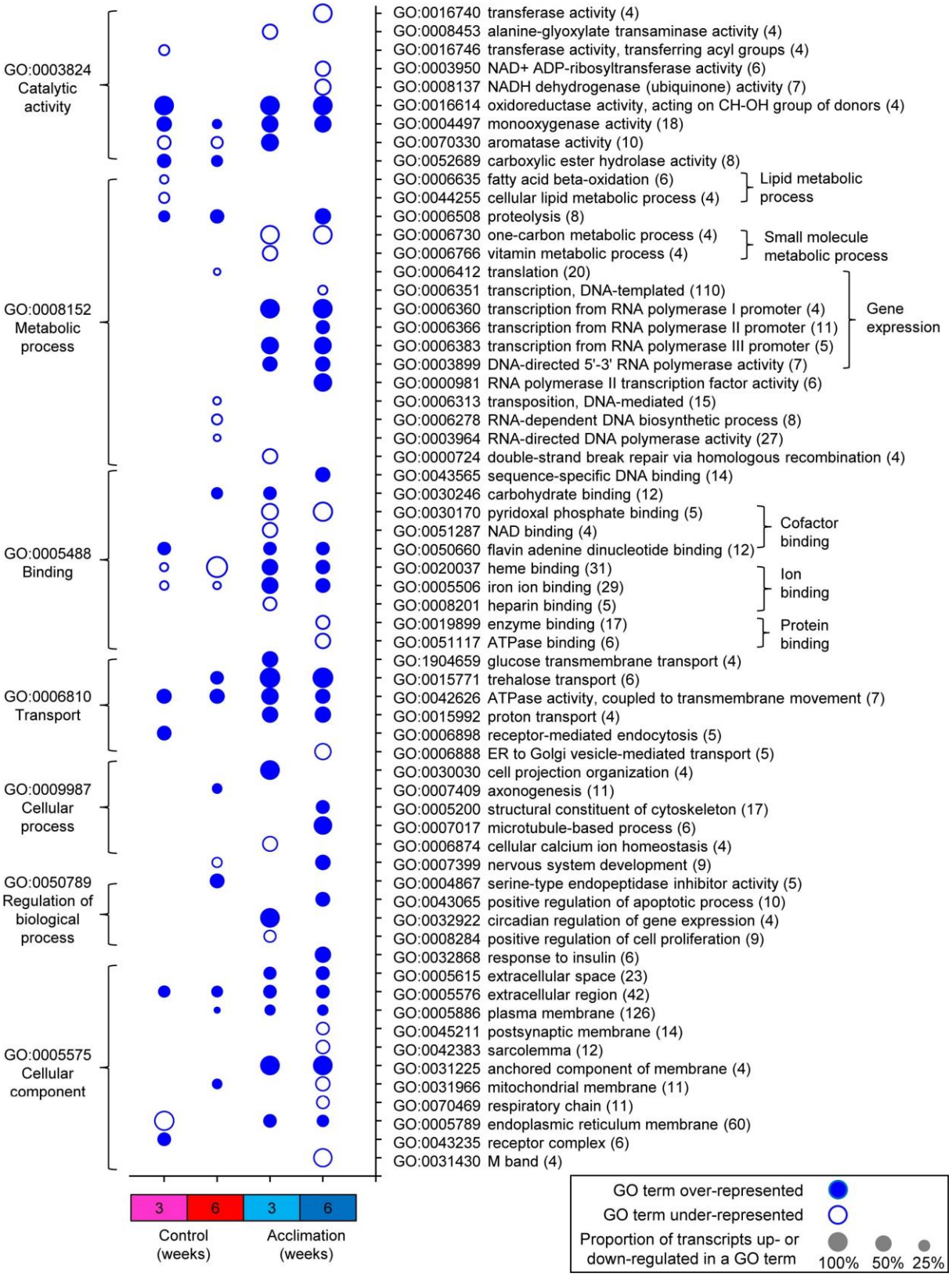
GO:0003824 Catalytic activity
GO:0008152 Metabolic process
GO:0005488 Binding
GO:0006810 Transport
GO:0009987 Cellular process
GO:0050789 Regulation of biological process
GO:0005575 Cellular component
GO:0016740 transferase activity (4)
GO:0008453 alanine-glyoxylate transaminase activity (4)
GO:0016746 transferase activity, transferring acyl groups (4)
GO:0003950 NAD+ ADP-ribosyltransferase activity (6)
GO:0008137 NADH dehydrogenase (ubiquinone) activity (7)
GO:0016614 oxidoreductase activity, acting on CH-OH group of donors (4)
GO:0004497 monooxygenase activity (18)
GO:0070330 aromatase activity (10)
GO:0052689 carboxylic ester hydrolase activity (8)
GO:0006635 fatty acid beta-oxidation (6)
GO:0044255 cellular lipid metabolic process (4)
Lipid metabolic process
GO:0006508 proteolysis (8)
GO:0006730 one-carbon metabolic process (4)
GO:0006766 vitamin metabolic process (4)
Small molecule metabolic process
GO:0006412 translation (20)
GO:0006351 transcription, DNA-templated (110)
GO:0006360 transcription from RNA polymerase I promoter (4)
GO:0006366 transcription from RNA polymerase II promoter (11)
GO:0006383 transcription from RNA polymerase III promoter (5)
GO:0003899 DNA-directed 5'-3' RNA polymerase activity (7)
Gene expression
GO:0000981 RNA polymerase II transcription factor activity (6)
GO:0006313 transposition, DNA-mediated (15)
GO:0006278 RNA-dependent DNA biosynthetic process (8)
GO:0003964 RNA-directed DNA polymerase activity (27)
GO:0000724 double-strand break repair via homologous recombination (4)
GO:0043565 sequence-specific DNA binding (14)
GO:0030246 carbohydrate binding (12)
GO:0030170 pyridoxal phosphate binding (5)
GO:0051287 NAD binding (4)
GO:0050660 flavin adenine dinucleotide binding (12)
Cofactor binding
GO:0020037 heme binding (31)
GO:0005506 iron ion binding (29)
GO:0008201 heparin binding (5)
Ion binding
GO:0019899 enzyme binding (17)
GO:0051117 ATPase binding (6)
Protein binding
GO:1904659 glucose transmembrane transport (4)
GO:0015771 trehalose transport (6)
GO:0042626 ATPase activity, coupled to transmembrane movement (7)
GO:0015992 proton transport (4)
GO:0006898 receptor-mediated endocytosis (5)
GO:0006888 ER to Golgi vesicle-mediated transport (5)
GO:0030030 cell projection organization (4)
GO:0007409 axonogenesis (11)
GO:0005200 structural constituent of cytoskeleton (17)
GO:0007017 microtubule-based process (6)
GO:0006874 cellular calcium ion homeostasis (4)
GO:0007399 nervous system development (9)
GO:0004867 serine-type endopeptidase inhibitor activity (5)
GO:0043065 positive regulation of apoptotic process (10)
GO:0032922 circadian regulation of gene expression (4)
GO:0008284 positive regulation of cell proliferation (9)
GO:0032868 response to insulin (6)
GO:0005615 extracellular space (23)
GO:0005576 extracellular region (42)
GO:0005886 plasma membrane (126)
GO:0045211 postsynaptic membrane (14)
GO:0042383 sarcolemma (12)
GO:0031225 anchored component of membrane (4)
GO:0031966 mitochondrial membrane (11)
GO:0070469 respiratory chain (11)
GO:0005789 endoplasmic reticulum membrane (60)
GO:0043235 receptor complex (6)
GO:0031430 M band (4)
3
6
3
6
Control (weeks)
Acclimation (weeks)
GO term over-represented
GO term under-represented
Proportion of transcripts up- or down-regulated in a GO term
100%
50%
25%

Figure 3


4
0
-4
GAGE test statistic
Control-3 wk
Control-6 wk
Acclimation-3 wk
Acclimation-6 wk
1 2 3 1 2 3 1 2 3 1 2 3
Upregulated relative to control week 0
ko03320 PPAR signaling pathway
ko03030 DNA replication
ko04062 Chemokine signaling pathway
ko04110 Cell cycle
ko04142 Lysosome
ko04144 Endocytosis
ko04151 PI3K-Akt signaling pathway
ko04360 Axon guidance
ko04510 Focal adhesion
ko04512 ECM-receptor interaction
ko04015 Rap1 signaling pathway
ko04013 MAPK signaling pathway - fly
Downregulated relative to control week 0
ko00030 Pentose phosphate pathway
ko00270 Cysteine and methionine metabolism
ko00520 Amino sugar and nucleotide sugar metabolism
ko04146 Peroxisome
ko00250 Alanine, aspartate and glutamate metabolism
ko01120 Microbial metabolism in diverse environments
ko01110 Biosynthesis of secondary metabolites
ko01230 Biosynthesis of amino acids
ko03040 Spliceosome
ko03010 Ribosome
ko03013 RNA transport
ko03020 RNA polymerase
ko04260 Cardiac muscle contraction
ko03060 Protein export
ko00970 Aminoacyl-tRNA biosynthesis
ko00190 Oxidative phosphorylation
ko03008 Ribosome biogenesis in eukaryotes

626 **Figure 4**

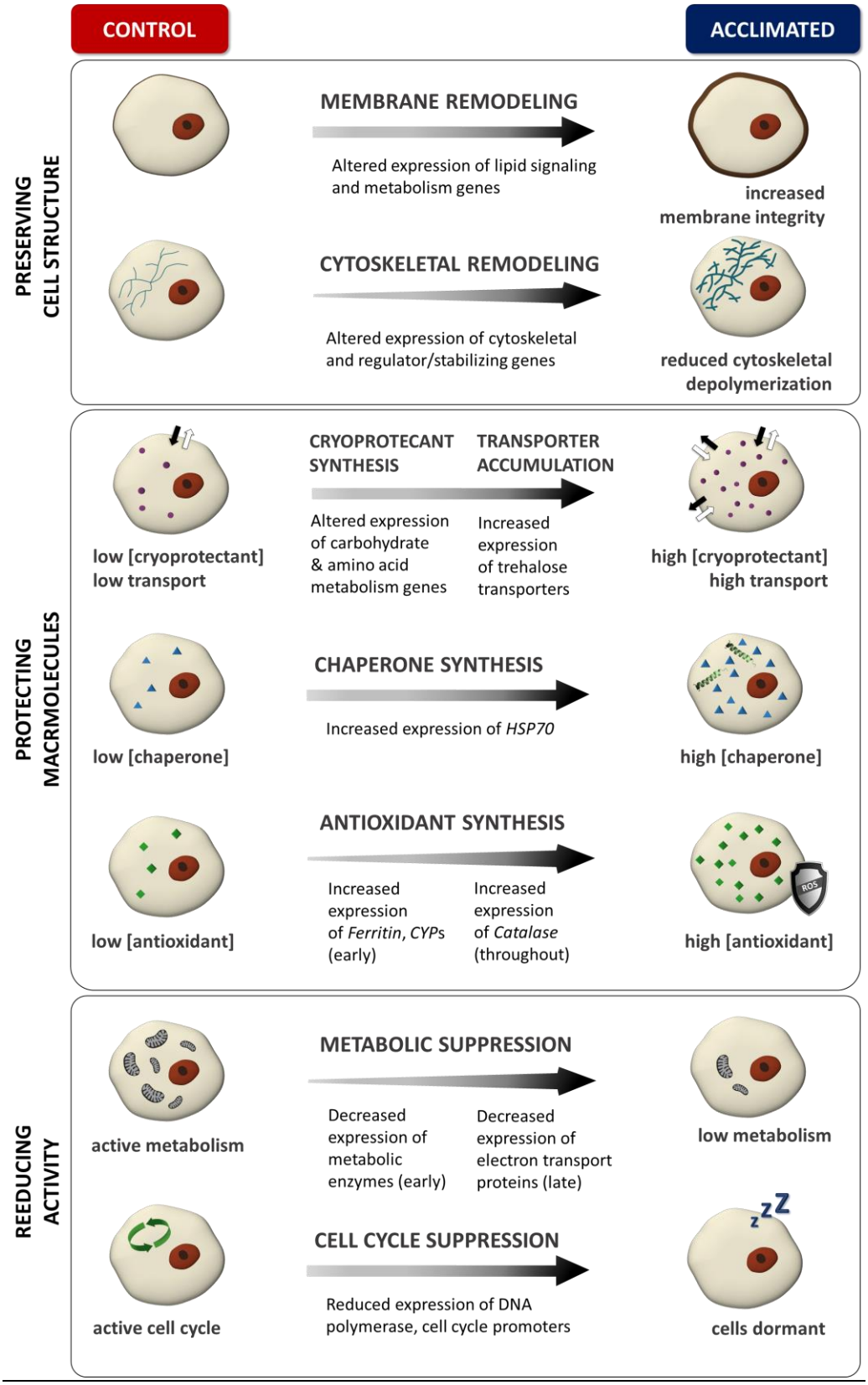

627

Supplementary Tables

Table S1. Selected transcripts of interest that were not differentially expressed in *Gryllus veletis* fat body during acclimation.

Function	Description	Contig ID
Potential cryoprotectant synthesis enzymes		
Inositol synthesis	Inositol-P synthase	Gvel_56451_c5_g2
Proline synthesis	P5C synthase	Gvel_66589_c0_g1
	P5C reductase	Gvel_69512_c0_g1
Trehalose synthesis	Bifunctional T6P synthase/phosphatase	Gvel_54376_c0_g1
Glycogen breakdown	Glycogen phosphorylase	Gvel_23709_c0_g1
	Glycogen phosphorylase	Gvel_38846_c0_g1
	Glycogen phosphorylase	Gvel_50699_c0_g1
Potential cryoprotectant transporters		
Proline transport	Sodium-dependent neutral amino acid transporter B(0)AT2	Gvel_26522_c1_g1
	Proton-coupled amino acid transporter 4	Gvel_42160_c0_g1
	Proton-coupled amino acid transporter 4	Gvel_73282_c0_g1
myo-Inositol transport	GPI inositol-deacylase	Gvel_10568_c0_g1
General amino acid transport		
	Putative sodium-coupled neutral amino acid transporter 7	Gvel_83253_c2_g1
	Sodium-coupled neutral amino acid transporter 9 homolog	Gvel_69575_c0_g1
	Sodium-dependent neutral amino acid transporter B(0)AT1	Gvel_74286_c0_g1
	Sodium-dependent neutral amino acid transporter B(0)AT3	Gvel_17082_c0_g1
	Putative sodium-coupled neutral amino acid transporter 11	Gvel_78773_c1_g1
	Proton-coupled amino acid transporter 4	Gvel_17696_c0_g1
	Proton-coupled amino acid transporter 4	Gvel_18085_c0_g1
	Proton-coupled amino acid transporter 4	Gvel_25506_c0_g1
	Proton-coupled amino acid transporter 4	Gvel_25679_c0_g1
	Proton-coupled amino acid transporter 4	Gvel_26291_c0_g1
	Proton-coupled amino acid transporter 4	Gvel_56726_c0_g1
	Amino acid transporter ANTL1	Gvel_19506_c0_g1
	b(0,+)-type amino acid transporter 1	Gvel_5247_c0_g1
	b(0,+)-type amino acid transporter 1	Gvel_42656_c0_g1
	b(0,+)-type amino acid transporter 1	Gvel_41737_c0_g1
	High affinity cationic amino acid transporter 1	Gvel_13471_c0_g1
	High affinity cationic amino acid transporter 1	Gvel_32998_c0_g1
	High affinity cationic amino acid transporter 1	Gvel_72649_c0_g1
	High affinity cationic amino acid transporter 1	Gvel_73575_c0_g1
	High affinity cationic amino acid transporter 1	Gvel_26563_c0_g1

635 **Table S1 continued**

Function	Description	Contig ID
	Cationic amino acid transporter 2	Gvel_5461_c0_g1
	Cationic amino acid transporter 2	Gvel_29535_c0_g1
	Cationic amino acid transporter 2	Gvel_73575_c0_g1
	Cationic amino acid transporter 3	Gvel_6717_c0_g2
	Cationic amino acid transporter 3	Gvel_58226_c0_g1
	Cationic amino acid transporter 4	Gvel_60049_c0_g1
	Excitatory amino acid transporter 3	Gvel_28987_c0_g2
	Sodium-dependent nutrient amino acid transporter 1	Gvel_66850_c0_g1
	Sodium-dependent nutrient amino acid transporter 1	Gvel_60491_c0_g1
Aquaporins		
Water transport	Aquaporin AQPcic	Gvel_37176_c0_g1
	Aquaporin AQPcic	Gvel_46914_c0_g1
	Aquaporin AQPAe	Gvel_51308_c1_g1
	Aquaporin-12	Gvel_56044_c0_g1
Molecular Chaperones		
Heat shock proteins	10 kDa heat shock protein, mitochondrial	Gvel_78446_c0_g1_i1
	60 kDa heat shock protein, mitochondrial	Gvel_27658_c0_g1_i1
	60 kDa heat shock protein, mitochondrial	Gvel_56040_c0_g1_i1
	Heat shock protein 67B2	Gvel_79017_c0_g1_i1
	Heat shock protein HSP 90-alpha A2	Gvel_28035_c0_g1_i1
	Heat shock protein HSP 90-alpha	Gvel_68127_c0_g1_i1
	Heat shock protein Hsp-16.2	Gvel_37784_c0_g2_i1
	Heat shock protein Hsp-16.2	Gvel_37784_c0_g1_i1
	Heat shock protein 70	Gvel_78482_c1_g1_i1
	Heat shock 70 kDa protein	Gvel_78482_c2_g1_i1
	Heat shock cognate 70 kDa protein	Gvel_9203_c0_g1_i1
	Heat shock 70 kDa protein	Gvel_57949_c0_g3_i1
	Major heat shock 70 kDa protein Ab	Gvel_16103_c0_g1_i1
	Heat shock 70 kDa protein 1	Gvel_18794_c0_g1_i1
	Heat shock protein 70 B2	Gvel_61233_c0_g1_i1
	Heat shock protein 70 B2	Gvel_83898_c0_g1_i1
	Heat shock 70 kDa protein 4	Gvel_87722_c0_g1_i1
	Heat shock 70 kDa protein 4	Gvel_87722_c0_g1_i2
	Heat shock 70 kDa protein A	Gvel_57949_c0_g1_i1
	Heat shock 70 kDa protein A	Gvel_57949_c0_g2_i1
	Heat shock 70 kDa protein cognate 1	Gvel_60996_c0_g2_i1
	Heat shock 70 kDa protein cognate 2	Gvel_78482_c0_g1_i1
	Heat shock 70 kDa protein cognate 2	Gvel_19946_c0_g1_i1
	Heat shock cognate 71 kDa protein	Gvel_12474_c0_g1_i1

636
637

638 **Table S1 continued**

639

Function	Description	Contig ID
	Heat shock 70 kDa protein cognate 3	Gvel_60796_c0_g1_i1
	Heat shock 70 kDa protein cognate 3	Gvel_78480_c0_g1_i2
	Heat shock 70 kDa protein cognate 3	Gvel_78480_c0_g1_i1
	Heat shock 70 kDa protein cognate 3	Gvel_78770_c0_g1_i1
	Heat shock cognate 71 kDa protein	Gvel_22440_c0_g1_i1
	Heat shock 70 kDa protein cognate 4	Gvel_34771_c0_g1_i1
	Heat shock 70 kDa protein cognate 4	Gvel_31684_c0_g1_i1
	Heat shock 70 kDa protein 14	Gvel_57508_c0_g1_i1
	Heat shock 70 kDa protein cognate 5	Gvel_51846_c0_g1_i1
	Heat shock 70 kDa protein cognate 5	Gvel_78850_c0_g1_i1
	Heat shock protein 83	Gvel_18505_c0_g1_i1
	Heat shock protein 83	Gvel_76432_c0_g1_i1
	Heat shock protein 83	Gvel_26469_c4_g9_i1
	Heat shock protein 90	Gvel_6014_c0_g1_i1
	Heat shock protein 75 kDa, mitochondrial	Gvel_87650_c0_g1_i1

640

641

642 **Table S2. Selected transcripts upregulated in *Gryllus veletis* fat body during acclimation, in**
643 **addition to those discussed in the text.**
644

Function	Description	Contig ID	Pattern
Putative ice binding proteins[a]			
C-type lectin domain protein	Hemolymph lipopolysaccharide-binding protein	Gvel_14378_c0_g1_i1	E
	Hemolymph lipopolysaccharide-binding protein	Gvel_73626_c0_g1_i2	E
	Hemolymph lipopolysaccharide-binding protein	Gvel_15098_c0_g1_i1	H
Putative transcription factors[b]			
General	ATP-dependent RNA helicase DHX36	Gvel_85658_c0_g2_i1	B
	CCHC-type zinc finger protein CG3800	Gvel_73663_c0_g1_i1	C
	CCHC-type zinc finger protein CG3800	Gvel_48092_c0_g1_i1	D
	Chorion transcription factor Cf2	Gvel_30148_c2_g1_i1	G
	Chromodomain-helicase-DNA-binding protein 1	Gvel_62761_c0_g1_i1	D
	CREB/ATF bZIP transcription factor	Gvel_22640_c0_g1_i1	C
	CXXC-type zinc finger protein 1	Gvel_82026_c0_g2_i1	G
	DNA-binding protein D-ETS-4	Gvel_16617_c0_g1_i1	H
	DNA-binding protein Ets97D	Gvel_35132_c0_g1_i1	D
	Gastrula zinc finger protein XlCGF26.1	Gvel_8013_c0_g2_i1	B
	Gastrula zinc finger protein XlCGF57.1	Gvel_44855_c2_g2_i1	G
	Gastrula zinc finger protein XlCGF57.1	Gvel_30226_c5_g4_i1	A
	General transcription factor IIE subunit 1	Gvel_62557_c0_g2_i1	D
	General transcription factor IIH subunit 1	Gvel_63875_c0_g1_i2	D
	General transcription factor IIH subunit 1	Gvel_63875_c0_g1_i3	E
	General transcription factor IIH subunit 4	Gvel_41185_c0_g1_i1	C
	Mediator of RNA polymerase II transcription subunit 13	Gvel_39856_c1_g1_i1	H
	Mediator of RNA polymerase II transcription s subunit 26	Gvel_43951_c0_g2_i1	C
	Mushroom body large-type Kenyon cell-specific protein 1	Gvel_55728_c0_g1_i1	E
	NFX1-type zinc finger-containing protein 1	Gvel_51372_c0_g1_i2	A
	Nucleolar transcription factor 1	Gvel_19437_c0_g1_i2	B
	RB-associated KRAB zinc finger protein	Gvel_53258_c0_g2_i1	B
	SAM pointed domain-containing Ets transcription factor	Gvel_22687_c0_g1_i2	H
	Transcription factor GATA-4	Gvel_33512_c0_g1_i1	H
	Transcription factor SOX-5	Gvel_70660_c0_g1_i1	H
	WD repeat-containing protein 43	Gvel_17203_c0_g1_i1	D
	Zinc finger MYND domain-containing protein 11	Gvel_78950_c0_g2_i1	C
	Zinc finger protein 26	Gvel_67773_c0_g1_i1	G
	Zinc finger protein 79	Gvel_78746_c1_g3_i1	A
	Zinc finger protein 84	Gvel_70614_c0_g1_i1	A
	Zinc finger protein 84	Gvel_50214_c1_g1_i1	B
	Zinc finger protein 84	Gvel_30148_c1_g1_i1	G
	Zinc finger protein 182	Gvel_44834_c8_g7_i1	A

645 **Table S2 continued**
646

Function	Description	Contig ID	Pattern
	Zinc finger protein 271	Gvel_80211_c1_g1_i1	A
	Zinc finger protein 330 homolog	Gvel_79200_c1_g1_i2	B
	Zinc finger protein 391	Gvel_70172_c3_g6_i1	D
	Zinc finger protein 425	Gvel_23073_c0_g1_i1	H
	Zinc finger protein 436	Gvel_67274_c0_g1_i2	A
	Zinc finger protein 436	Gvel_4482_c0_g1_i2	D
	Zinc finger protein 583	Gvel_30226_c5_g12_i2	A
	Zinc finger protein 652	Gvel_64997_c0_g1_i1	A
	Zinc finger protein 658	Gvel_47218_c0_g1_i1	A
	Zinc finger protein 706	Gvel_88016_c0_g1_i1	C
	Zinc finger protein basonuclin-2	Gvel_78940_c0_g1_i1	H
	Zinc finger protein jing homolog	Gvel_41632_c0_g1_i1	E
	Zinc finger protein ush	Gvel_24964_c0_g1_i1	H
	Zinc finger protein Xfin	Gvel_44802_c0_g1_i1	B
Response to Stress	Forkhead box protein L2	Gvel_41282_c0_g1_i2	H
	Metal regulatory transcription factor 1	Gvel_51888_c0_g1_i1	D
	Homeodomain-interacting protein kinase 2	Gvel_46976_c1_g1_i1	B
	Homeodomain-interacting protein kinase 2	Gvel_46976_c1_g1_i2	H
Cell Cycle/Apotosis	LIM domain-containing protein jub	Gvel_63855_c0_g1_i2	H
	Max-binding protein MNT	Gvel_54552_c0_g1_i1	E
	HMG box-containing protein 1	Gvel_80210_c0_g4_i2	A
	Transcription factor kayak	Gvel_55714_c0_g1_i1	G
	Transcription factor kayak	Gvel_55714_c0_g1_i3	H
	Transcriptional repressor CTCF	Gvel_84806_c0_g1_i1	D
	Zinc finger HIT domain-containing protein 1	Gvel_82020_c0_g1_i1	C
	Homeodomain-interacting protein kinase 2	Gvel_46976_c1_g1_i1	B
	Homeodomain-interacting protein kinase 2	Gvel_46976_c1_g1_i2	H
RNA Processing	ATP-dependent RNA helicase DHX8	Gvel_62756_c0_g1_i1	G
	ATP-dependent RNA helicase p62	Gvel_49169_c0_g1_i1	C
	ATP-dependent RNA helicase p62	Gvel_49169_c0_g1_i2	D
	Box C/D snoRNA protein 1	Gvel_63966_c0_g1_i2	D
	LIM and calponin homology domains-containing protein 1	Gvel_82488_c0_g1_i3	H
	Peptidylprolyl isomerase domain and WD repeat-containing protein 1	Gvel_80573_c0_g1_i1	C
	Probable ATP-dependent RNA helicase DDX5	Gvel_82013_c0_g1_i3	C
	Probable ATP-dependent RNA helicase DDX17	Gvel_37175_c0_g1_i2	E
	Probable ATP-dependent RNA helicase DDX46	Gvel_81996_c0_g3_i1	E
	Probable ATP-dependent RNA helicase DHX35	Gvel_32073_c0_g1_i1	E
	WD repeat-containing protein 36	Gvel_63749_c0_g1_i2	D
	WD repeat-containing protein 37	Gvel_62586_c0_g1_i1	E
	Zinc finger CCCH domain-containing protein 13	Gvel_15051_c0_g1_i1	D

647 **Table S2 continued**
648

Function	Description	Contig ID	Pattern
Ubiquitination	Zinc finger protein 36, C3H1 type-like 1	Gvel_35319_c0_g1_i1	D
	Ankyrin repeat and SOCS box protein 8	Gvel_70174_c8_g9_i1	B
	Ankyrin repeat and SOCS box protein 8	Gvel_70174_c8_g9_i2	C
	CCR4-NOT transcription complex subunit 4	Gvel_35911_c1_g1_i3	A
	F-box only protein 9	Gvel_36722_c0_g1_i2	B
	F-box/LRR-repeat protein 7	Gvel_46226_c0_g1_i1	A
	F-box/WD repeat-containing protein 1A	Gvel_41154_c0_g1_i3	B
	F-box/WD repeat-containing protein 4	Gvel_68222_c0_g2_i1	B
	RING-box protein 1A	Gvel_4127_c0_g1_i1	C
	SPRY domain-containing SOCS box protein 3	Gvel_54345_c0_g1_i4	A
Other	WD repeat-containing protein 11	Gvel_25027_c0_g1_i3	B
	Glutamate-rich WD repeat-containing protein 1	Gvel_84817_c0_g1_i1	C
	Probable ATP-dependent RNA helicase DDX28	Gvel_23096_c0_g1_i1	D
	Protein cycle	Gvel_46912_c0_g1_i2	E
	Signal transducer and activator of transcription 5B	Gvel_23665_c0_g1_i4	C
Putative signalling transduction genes[c]			
General	Homeodomain-interacting protein kinase 2	Gvel_46976_c1_g1_i2	H
	Homeodomain-interacting protein kinase 2	Gvel_46976_c1_g1_i1	B
	Serine/threonine-protein phosphatase 5	Gvel_61181_c0_g1_i1	A
	Serine/threonine-protein phosphatase PP1-beta catalytic subunit	Gvel_48735_c0_g2_i1	E
Metabolism	5'-AMP-activated protein kinase subunit gamma-2	Gvel_61474_c0_g1_i1	E
	Adiponectin receptor protein	Gvel_46799_c0_g1_i1	B
	FGGY carbohydrate kinase domain-containing protein	Gvel_51886_c0_g2_i1	C
	Tyrosine-protein phosphatase non-receptor type 23	Gvel_85672_c0_g1_i2	D
	Scavenger receptor class B member 1	Gvel_70834_c0_g1_i1	B
	Serine/threonine-protein phosphatase 2A 65 kDa regulatory subunit A alpha isoform	Gvel_46757_c0_g1_i2	A
	Serine/threonine-protein phosphatase 2A catalytic subunit alpha isoform	Gvel_45193_c0_g1_i1	H
Insulin signalling	3-phosphoinositide-dependent protein kinase 1	Gvel_8541_c0_g1_i1	G
	3-phosphoinositide-dependent protein kinase 1	Gvel_85409_c0_g1_i1	E
Cell cycle/Apoptosis	CDK-activating kinase assembly factor MAT1	Gvel_21437_c0_g1_i1	C
	Dual specificity protein phosphatase 10	Gvel_34643_c0_g1_i1	H
	Death-associated protein kinase 1	Gvel_79256_c0_g1_i1	A
	Kinase D-interacting substrate of 220 kDa	Gvel_44786_c3_g1_i1	E
	Kinase D-interacting substrate of 220 kDa	Gvel_70232_c1_g1_i1	A
	Mitogen-activated protein kinase 14A	Gvel_17318_c0_g1_i2	B
	NUAK family SNF1-like kinase 1	Gvel_37649_c0_g1_i1	B
	Ras GTPase-activating protein 1	Gvel_17341_c0_g1_i2	B
	Transforming growth factor-beta receptor-associated protein 1	Gvel_47003_c0_g1_i1	A
	Serine/threonine-protein phosphatase 1 regulatory subunit 10	Gvel_19509_c1_g1_i2	C

Table S2 continued

Function	Description	Contig ID	Pattern
Cytoskeleton	EGFR kinase substrate 8-like protein 2	Gvel_43838_c0_g1_i1	B
	Ras GTPase-activating protein 1	Gvel_17341_c0_g1_i2	B
	Rho GTPase-activating protein 100F	Gvel_4601_c0_g1_i1	H
	Serine/threonine-protein kinase OSR1	Gvel_48744_c1_g1_i1	E
	Serine/threonine-protein phosphatase 2A 65 kDa regulatory subunit A alpha isoform	Gvel_46757_c0_g1_i2	A
	Serine/threonine-protein phosphatase 2A catalytic subunit alpha isoform	Gvel_45193_c0_g1_i1	H
	Tyrosine-protein kinase Src64B	Gvel_81960_c0_g1_i1	B
Stress response	G-protein coupled receptor Mth	Gvel_35842_c0_g1_i1	H
	G-protein coupled receptor Mth2	Gvel_27887_c0_g1_i1	E
	Stress-activated protein kinase JNK	Gvel_49939_c0_g1_i1	A
	Serine/threonine-protein kinase OSR1	Gvel_48744_c1_g1_i1	E
RNA processing	Serine/threonine-protein kinase Doa	Gvel_62201_c0_g3_i2	H
	Serine/threonine-protein kinase Doa	Gvel_62201_c0_g2_i1	D
	Serine/threonine-protein kinase SMG1	Gvel_19473_c0_g2_i2	C
cAMP signalling	Adenylate cyclase type 5	Gvel_28980_c0_g4_i4	D
	Metabotropic glutamate receptor 3	Gvel_3867_c0_g1_i1	A
	Protein kinase DC2	Gvel_84502_c0_g1_i1	H
Inositol signalling	Inositol 1,4,5-trisphosphate receptor	Gvel_41178_c0_g4_i1	B
	Inositol-trisphosphate 3-kinase A	Gvel_87759_c0_g1_i1	H
	Phosphatidylinositol 5-phosphate 4-kinase type-2 alpha	Gvel_53190_c0_g1_i1	B
	Phosphatidylinositol phosphatase PTPRQ	Gvel_80174_c5_g1_i1	A
	Tyrosine-protein phosphatase non-receptor type 13	Gvel_70163_c1_g1_i1	B
Immune	Inhibitor of nuclear factor kappa-B kinase subunit alpha	Gvel_31546_c0_g1_i1	A
	Interleukin-1 receptor-associated kinase 4	Gvel_62503_c0_g1_i1	C
	Protein toll	Gvel_60975_c0_g1_i1	E
	Serine/threonine-protein kinase RIO3	Gvel_73695_c0_g1_i1	G
	Src kinase-associated phosphoprotein 2-A	Gvel_88116_c0_g1_i1	A
Vesicles	ADP-ribosylation factor GTPase-activating protein 1	Gvel_27359_c0_g1_i1	A
	Low-density lipoprotein receptor-related protein 1B	Gvel_65167_c0_g1_i1	B
	Prolow-density lipoprotein receptor-related protein 1	Gvel_78586_c0_g1_i1	B
Autophagy	Phosphoinositide 3-kinase regulatory subunit 4	Gvel_64764_c0_g1_i1	D
	Rab3 GTPase-activating protein non-catalytic subunit	Gvel_51317_c0_g2_i2	A
Other	Serine/threonine-protein kinase Sgk3	Gvel_84125_c0_g1_i2	B
	Tankyrase	Gvel_41304_c0_g1_i1	E
	UMP-CMP kinase 2, mitochondrial	Gvel_32063_c0_g1_i1	C

[a]Transcripts with homology to C-type lectins (homologous to fish antifreeze proteins), Pfam domain PF00059. Two putative sialic acid synthase (homologous to fish antifreeze proteins), Pfam domain PF08666 were not differentially expressed;
[b]Transcript names that include: 'box,' 'DNA-binding,' 'homeodomain,' 'LIM domain,' 'RNA' (excluding polymerases, RNA binding proteins, tRNA),'transcription,' 'WD repeat,' 'zinc;'
[c]Transcript names that include: 'cyclase,' 'G-protein,' 'GTPase,' 'kinase,' 'phosphatase' (excluding biochemical pathway kinases and phosphatases), 'receptor' (excluding organelle level receptors, PPAR signalling).

Table S3. Selected transcripts of interest whose transcripts were abundant, but not differentially expressed, in *Gryllus veletis* fat body during acclimation. '--NA--' indicates the transcript is unannotated.

Description	Contig ID	Transcript count[a]
Transferrin	Gvel_70215_c1_g7_i1	1,094,891
Transferrin	Gvel_70215_c1_g4_i1	680,004
--NA--	Gvel_37243_c0_g2_i1	657,095
Putative uncharacterized protein ART2	Gvel_53547_c0_g1_i1	642,521
Phosphoenolpyruvate carboxykinase [GTP]	Gvel_47855_c0_g2_i1	641,599
Acyl-CoA Delta(11) desaturase	Gvel_54359_c1_g1_i2	493,723
Carboxypeptidase N subunit 2	Gvel_61067_c0_g1_i1	444,731
--NA--	Gvel_31776_c0_g1_i1	370,799
Elongation factor 2	Gvel_9392_c0_g1_i1	358,856
Cytochrome P450 4C1	Gvel_66551_c6_g2_i1	352,700
--NA--	Gvel_70215_c1_g5_i1	313,522
Heat shock 70 kDa protein cognate 4	Gvel_34771_c0_g1_i1	253,490
Hemolymph lipopolysaccharide-binding protein	Gvel_57983_c0_g1_i1	232,161
3-ketoacyl-CoA thiolase, mitochondrial	Gvel_62183_c0_g2_i1	214,886
Myosin heavy chain, muscle	Gvel_62487_c0_g1_i1	180,653
--NA--	Gvel_32829_c0_g1_i1	161,287
Probable phospholipid hydroperoxide glutathione peroxidase	Gvel_65566_c0_g1_i1	144,136
Probable medium-chain specific acyl-CoA dehydrogenase	Gvel_18079_c0_g1_i1	137,974
--NA--	Gvel_35884_c1_g1_i1	134,723
Delta(24)-sterol reductase	Gvel_84826_c0_g1_i1	133,590
--NA--	Gvel_75329_c0_g1_i1	124,759
--NA--	Gvel_52219_c0_g1_i1	124,207
Clavesin-1	Gvel_51746_c0_g1_i1	123,962
Glycerol-3-phosphate dehydrogenase [NAD(+)], cytoplasmic	Gvel_82643_c0_g2_i1	123,713
Long-chain-fatty-acid--CoA ligase 5	Gvel_3925_c0_g1_i1	121,244
Bifunctional trehalose-6-phosphate synthase/phosphatase	Gvel_54376_c0_g1_i1	119,317
ATP-binding cassette sub-family G member 1	Gvel_44596_c0_g2_i1	115,246
Very low-density lipoprotein receptor	Gvel_82464_c0_g1_i1	115,013
Glutathione peroxidase	Gvel_12774_c0_g1_i1	113,014
Catalase	Gvel_54149_c0_g1_i1	111,760
40S ribosomal protein S2	Gvel_87148_c0_g1_i1	104,344
Long-chain-fatty-acid--CoA ligase 3	Gvel_57805_c1_g1_i1	101,293
--NA--	Gvel_24150_c0_g1_i1	100,799

[a]Sum of transcript read counts across three biological replicates of acclimated crickets; each biological replicate includes fat body RNA from five freeze-tolerant *G. veletis* (acclimated for six weeks).

Supplementary Figures

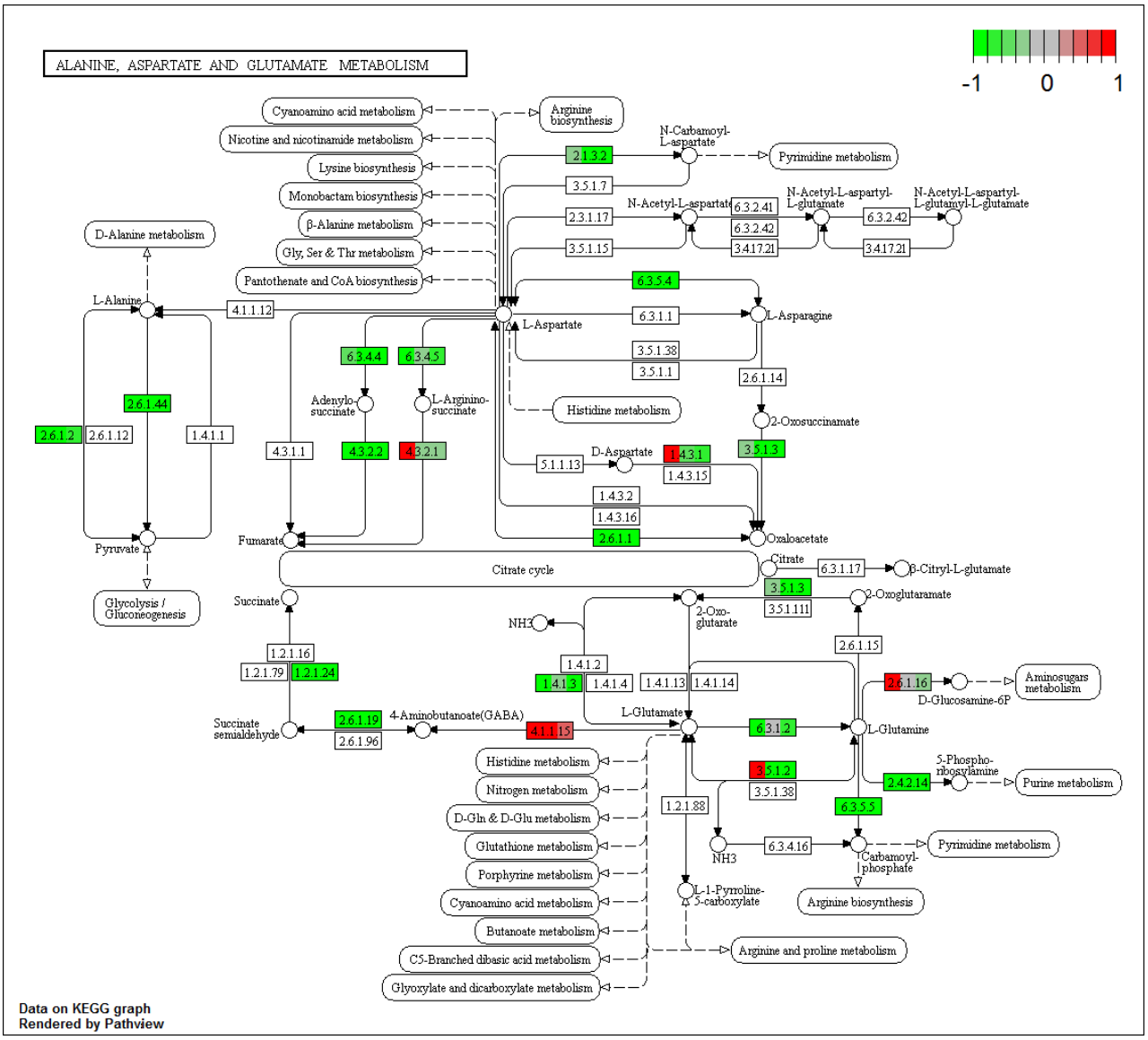

Figure S1 – Differential transcript expression in the 'alanine, aspartate and glutamate metabolism' KEGG pathway in G*ryllus veletis* acclimated for three weeks relative to zero-week controls. Each pathway component contains three colour bars indicating the three biological replicates of crickets acclimated for three weeks compared to the mean expression of control crickets (week zero), with red indicating increased expression, and green indicating decreased expression. 2.6.1.1 - aspartate transaminase; 2.6.1.2 - alanine transaminase; 2.6.1.44 - alanine-glyoxylate transaminase; 6.3.5.4 - asparagine synthase. For a complete description of each pathway component, see the KEGG 'alanine, aspartate and glutamate metabolism' reference pathway (http://www.genome.jp/kegg-bin/show_pathway?ko00250).

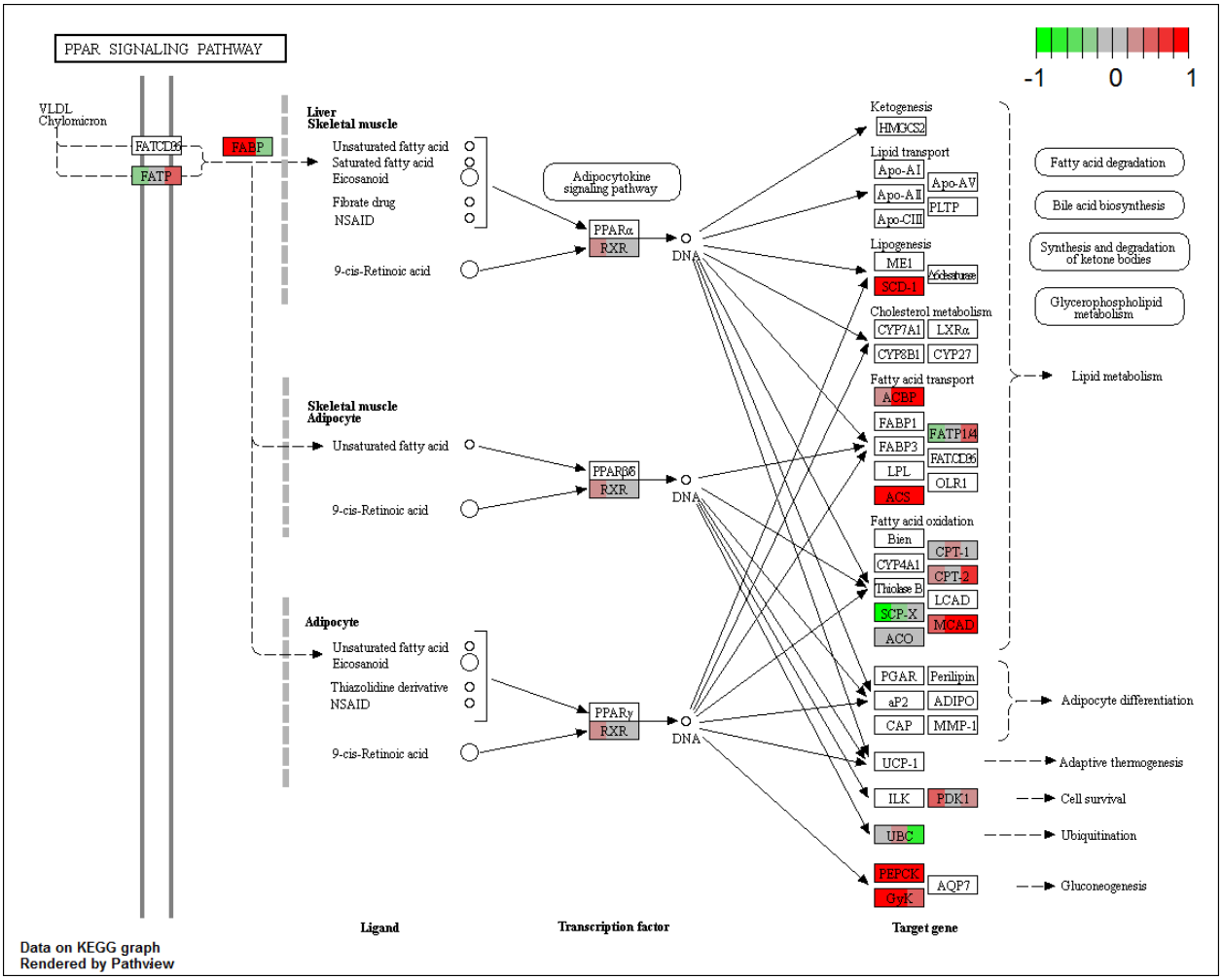

Figure S2 – Differential transcript expression in the 'PPAR signaling' KEGG pathway in *Gryllus veletis* acclimated for six weeks relative to zero-week controls. Each pathway component contains three colour bars indicating the three biological replicates of crickets acclimated for six weeks compared to the mean expression of control crickets (week zero), with red indicating increased expression, and green indicating decreased expression. GyK, glycerol kinase; MCAD, medium chain acyl-CoA dehydrogenase; PEPCK, phosphoenol pyruvate carboxykinase; SCD, stearoyl-CoA desaturase (SCD). For a complete description of each pathway component, see the KEGG 'PPAR signaling pathway' reference pathway (http://www.genome.jp/kegg-bin/show_pathway?ko03320)

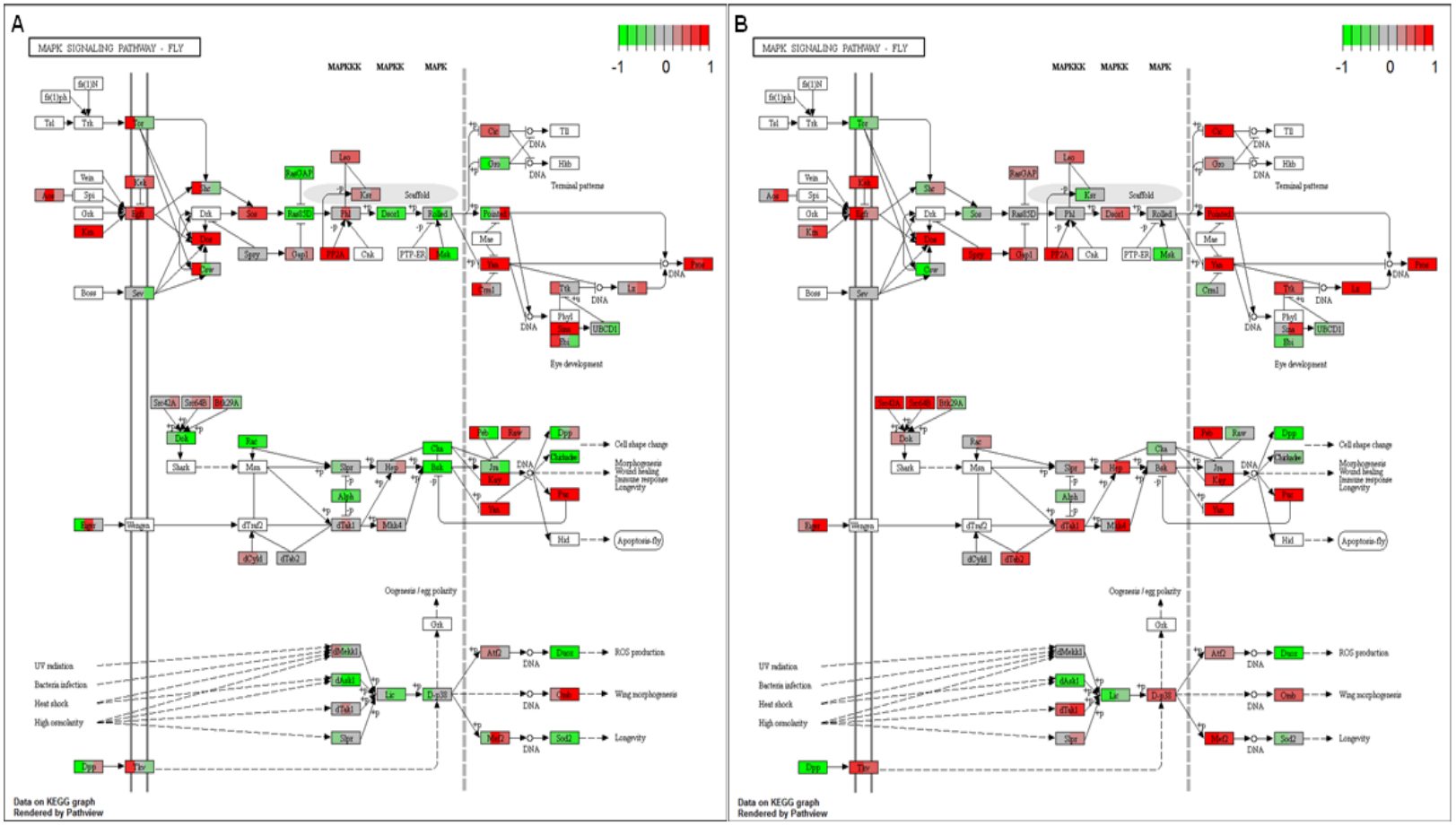

Figure S3 – Differential transcript expression in the 'MAPK signaling' KEGG pathway in *Gryllus veletis* (A) acclimated or (B) maintained under control conditions for six weeks relative to zero-week controls. Each pathway component contains three colour bars indicating the three biological replicates of crickets under acclimation or control conditions for six weeks compared to the mean expression of control crickets (week zero), with red indicating increased expression, and green indicating decreased expression. RasGAP, Ras GTPase activating protein. For a complete description of each pathway component, see the KEGG 'MAPK signaling' reference pathway (http://www.genome.jp/kegg-bin/show_pathway?ko04013)

693